2

Ultrasonic Characterisation of W/O Microemulsions – Structure, Phase Diagrams, State of Water in Nano–Droplets, Encapsulated Proteins, Enzymes

Vitaly Buckin and Shailesh Kumar Hallone
School of Chemistry & Chemical Biology, University College Dublin, Belfield, Dublin 4 Ireland

1. Introduction

The unique properties of microemulsions, such as stability, ease of preparation and their ability to form spontaneously have attracted considerable interest in numerous applications including, synthesis of polymers, delivery of active compounds, solubilisation of enzymes in organic solvents and biocatalysis. Developments of microemulsion based formulations require routine analytical techniques that allow users to analyse their microstructure and particle size, transitions between different phases and phase diagrams, the state of solutes encapsulated in microemulsion droplets and their activity (e.g. enzymes), and to monitor chemical reactions curried in microemulsions.

Ultrasonic spectroscopy has a considerable potential in this area as demonstrated previously (Lang et al., 1980; Ballaro et al., 1980; Zana et al., 1983; Cao et al., 1997; Mehta & Kawaljit, 1998; Wines et al., 1999; Letamendia et al., 2001). This technique employs an ultrasonic wave (MHz frequency range), which probes the elastic characteristics of materials. As it transverses a sample, compressions and decompressions in the ultrasonic wave change the distance between molecules within the sample, which in turn respond by intermolecular repulsions and attractions. This ability of ultrasonic waves to probe intermolecular forces allows access to molecular levels of organisation of materials. Measurements of scattering effects of ultrasonic waves provide particle size analysis. Application of ultrasonic spectroscopy in microemulsion systems in the past was often limited by the resolution of the measurements, requirements of large sample volumes and limited range of measuring regimes. Introduction of high-resolution ultrasonic spectroscopy (HR-US) (Buckin & O'Driscoll, 2002; Buckin et al., 2003; Kudryashov et al., 2000; Buckin et al., 2002) overcame the above limitations and allowed applications of this technique for analysis of microemulsion structure and phase diagrams (Hickey et al., 2006) in a simple automatic or manual titration regimes. The technique is based on precision measurements of ultrasonic velocity and attenuation in the frequency range 1 to 20MHz. In w/o microemulsions it provided characterization of transitions between different phases, such as swollen micelles, microemulsion, coarse emulsion, liquid crystals, and evaluation of microstructural attributes of the phases, as well as characterisation of the state of water in emulsion droplets and the

size of the droplets (Hickey et al., 2006, 2010). Previous applications of ultrasonic spectroscopy for analysis of microemulsions demonstrated an exceptional sensitivity of ultrasonic parameters to the structural characteristics of microemulsions and to the state of its components. However, utilisation of this information requires further developments of algorithms of processing of ultrasonic data and their relationship with microscopic and molecular characteristics of dispersions. One of the major focuses of this paper is interpretation of compressibility of microemulsions obtained from ultrasonic measurements. As a second derivative of thermodynamic potentials, compressibility is extremely sensitive to the state of components of complex mixtures. Compressibility represents the rigidity of the media, which is determined by intermolecular forces. In this sense, measurements of compressibility provide direct access to intermolecular interactions. As compression of medium is associated with energy transformations, including release of heat, compressibility is affected by the dynamics of this process, which in some cases results in its dependence of on the frequency or the time scale of the compression. This provides an additional tool for ultrasonic analysis of microstructural characteristics of mixtures and kinetics of molecular transformations. However, it also requires the correct theoretical algorithms for molecular interpretation of compressibility. The current paper combines the discussion of fundamental relationships between compressibility and structural and physical characteristics of microemulsions, and applications of these relationships for analysis of ultrasonic data on microemulsions, their microstructure and state of their components. Special attention was given to the assessment of the state of water in w/o microemulsion droplets, which plays a key role in regulation of the activity of water soluble ingredients encapsulated in the droplets (enzymes, drugs, etc.) and also to the algorithms for assessment of state of globular proteins encapsulated in w/o microemulsions. The results demonstrate that the ultrasonic technique allows efficient mapping of the areas of microemulsion phase diagrams with different states of water, including water in nano-droplets. The composition of microemulsion systems at the transition lines, surrounding the areas of presence of nano-droplets with well-defined water pool was correlated with the droplet size, obtained ultrasonically, and by other techniques. The 'upgraded' phase diagrams were used for successful (retaining of bioactivity) encapsulation of hydrolytic enzymes (e.g. cellobiase) in aqueous nano-droplets and for ultrasonic characterisation of enzyme activity in microemulsions.

2. Ultrasonic parameters and viscoelastic properties of liquids and gels

2.1 Ultrasonic wave and elasticity moduli

Ultrasonic wave is a wave of longitudinal deformations where compressions occur in direction of wave propagation. In isotropic materials, which are homogeneous within the scale of ultrasonic wave, the differential equation for a plain ultrasonic wave propagating over the axis x is given by (Litovitz & Davis, 1964; Thurston, 1964; Morse & Ingard, 1986; Powey, 1997):

$$\rho_I \frac{\partial^2 X}{\partial t^2} = M \frac{\partial^2 X}{\partial x^2} \tag{1}$$

where M is the longitudinal modulus of the medium, which represents the ratio of stress to strain in longitudinal deformation, X is the displacement of the medium at the point x, t is time, ρ_I is the effective inertial density of the medium, which represents the ratio between

the force applied to a small part of the liquid and the acceleration caused by the force. For homogeneous on microscopic level (length scale of the shear wave) liquids ρ_I is equal to the normal (gravimetric) density, for non- homogeneous liquids ρ_I deviates from the gravimetric density and depends on the frequency. The Equation (1) is valid for ultrasonic waves of small amplitude, e.g. relative longitudinal deformation in the wave, strain, is << 1. At this condition the speed of the wave is much higher than the speed of particles of the medium (Thurston, 1964).

The strain (deformation) may occur with some time delay relative to the stress applied. Incorporation of these effects for the case of harmonically oscillating stress is often done through representation of strain, stress and other associated variables (e.g. change of pressure, δP , temperature, δT , and volume, δV) as complex values given by $\mathbf{Z}e^{i\omega t}$,where $\mathbf{Z}\,(\equiv|\mathbf{Z}|e^{i\varphi_{\mathbf{Z}}}\equiv Z'+iZ''$, $|\mathbf{Z}|$ is the absolute amplitude and $\varphi_{\mathbf{Z}}$ the phase of $\mathbf{Z}$; Z' is the real and Z'' is the imaginary parts of $\mathbf{Z}$) is the complex amplitude of the corresponding parameter, $\omega\,(\equiv 2\pi f$, f is frequency of ultrasonic wave) is the angular frequency of oscillations, t is time, and $i\,(\equiv\sqrt{-1}\,)$ is the imaginary unit. In this case the longitudinal modulus can be represented by a complex constant, $\mathbf{M}\ \ (\equiv M'+iM'')$. The solution of Equation (1) in complex notations can be presented as $\mathbf{X}=\mathbf{X}_0e^{-\alpha x+i\omega(t-\frac{x}{u})}$ where $\mathbf{X}_0$ is the amplitude of the wave at $x=0$ and $t=0$, u is the ultrasonic velocity (phase speed of the wave) and α is the ultrasonic attenuation. If the elastic response dominates, $M'>>M''$ (often expressed as a small value of attenuation per wavelength, $\alpha\lambda<<1$, $\lambda=\frac{u}{f}$), which is correct for most of liquids and gels, the velocity and attenuation of ultrasonic wave are given as:

$$u=\sqrt{\frac{M'}{\rho_I}};\qquad\qquad \alpha=\frac{\omega M''}{2\rho_I u^3} \tag{2}$$

In the case of a medium, which consist of a liquid within a gel network, with the size of the networks comparable or exceeding the ultrasonic wavelength, the longitudinal module can be presented as a sum of contribution of the liquid, $\mathbf{M_{liquid}}$, and the gel, $\mathbf{M_{gel}}$, parts: $\mathbf{M}=\mathbf{M_{liquid}}+\mathbf{M_{gel}}$. The modulus of longitudinal deformation is a combination of the modulus of volume deformation, $\mathbf{K_V}(\equiv K_V'+iK_V'')$, and the modulus of shear deformation, $\mathbf{G}(\equiv G'+iG'')$ (see for example Litovitz & Davis, 1964): $\mathbf{M}=\mathbf{K_V}+\frac{4}{3}\mathbf{G}$. For most liquids the shear storage modulus, G'_{liquid}, is much smaller than the volume storage modulus, $K_V{}'_{liquid}$, ($G'_{liquid}<<K_V{}'_{liquid}$) and its contribution to M' in Equation (2) can be neglected.

It is often convenient to substitute the volume modulus of the liquid, $\mathbf{K_{V\,liquid}}$, by the coefficient of adiabatic compressibility of the liquid $\boldsymbol{\beta}\equiv\beta'+i\beta''\equiv\frac{1}{\mathbf{K_{V}}_{liquid}}$, which represents a relative change of the volume per unit of pressure applied: $\boldsymbol{\beta}\equiv-\frac{1}{V}\frac{\boldsymbol{\delta}\mathbf{V}}{\boldsymbol{\delta}\mathbf{P}}$. For $\frac{K_V{}'_{liquid}}{K_V{}''_{liquid}}>>1$

$$u = \sqrt{\frac{\frac{1}{\beta'} + M'_{gel}}{\rho_l}}; \qquad \alpha = \frac{\omega}{2\rho_l u^3}\left(-\frac{\beta''}{\beta'^2} + \frac{4}{3}G_{liquid}'' + M_{gel}''\right) \tag{3}$$

For liquids M'_{gel} and M''_{gel} shall be excluded from the above equations, which provides the well-known relationships for ultrasonic velocity: $u = \frac{1}{\sqrt{\beta'\rho_l}}$.

2.2 Compressibility and effects of heat exchange

Compression of a volume V caused by an applied pressure, δP, results in production of heat, which changes the temperature of the compressed volume by δT. The volume change, δV, caused by the applied pressure is a sum of two terms, compression of volume V at constant temperature, $\delta V_T = -K_T \delta P$, and the change of volume caused by its heat expansion at constant pressure, $\delta V_P = E\delta T$: $\delta V = \delta V_T + \delta V_P$, where K_T ($\equiv -\left(\frac{\delta V}{\delta P}\right)_T$) is the isothermal compressibility of volume V at constant temperature and E ($\equiv \left(\frac{\delta V}{\delta T}\right)_P$) is its heat expansibility at constant pressure. Therefore, the compressibility, K ($\equiv -\frac{\delta V}{\delta P}$), is given as $K = K_T - E\frac{\delta T}{\delta P}$.

The change of temperature δT is determined by the balance of the heat production in the compression of the volume V and the heat exchange between this volume and its environment. Two (major) processes of the heat exchange exist in the ultrasonic waves propagating through liquids. The first one is the heat flow between different parts of the ultrasonic wave, which have at any given time different compression and thus different temperature. The length scale of the volumes involved in heat exchange process is determined by the characteristics of the thermal wave, its wavelength, λ_T ($= \sqrt{\frac{4\pi\kappa}{f\rho c_P}}$, κ is the heat conductance of the medium, ρ is the gravimetric density) and is attenuation with distance $\sim e^{-\frac{x}{\delta_T}}$, where $\delta_T = \frac{\lambda_T}{2\pi}$ is the exponential decay length of the thermal wave. Therefore, the extent of the heat exchange within the ultrasonic wave is defined by the ratio of the wavelength of ultrasonic wave, λ, which controls the gradient of temperature within the wave and λ_T, which controls the length scale of the heat exchange during the time interval of compression. The functional dependence of the real and imaginary parts of compressibility (and ultrasonic velocity and attenuation) in ultrasonic waves in liquids on the ratio of λ_T to λ was analyzed previously (Thurston, 1964). Its application for such liquids as water or oils at room temperature shows that for ultrasonic frequencies, up to hundreds of MHz, the deviations of ultrasonic velocity and the real part of compressibility coefficient, β', from their values at pure adiabatic conditions of compression do not exceed 10^{-7} of their absolute values. This is negligible when compared with the existing limits of resolution in measurements of ultrasonic velocity. Thus, the compressibility of the media measured within normal ultrasonic frequency range, represents the adiabatic compressibility, K_S and the value of β' shall be taken as coefficient of adiabatic compressibility of the medium, β_S ($\equiv \frac{K_S}{V}$; $K_S \equiv -\left(\frac{\partial V}{\partial P}\right)_S$, S is entropy). The imaginary part of compressibility at this limit provides the well-known

equation for contribution to ultrasonic attenuation caused by the heat losses in homogeneous liquids, α_{TH}, (Pierce, 1991): $\alpha_{TH} = \omega^2 T \frac{\kappa e^2 \rho}{2uc_P^2}$, where e ($\equiv \frac{E}{m}$, m is the mass of the volume V) is the specific thermal expansibility of the medium.

The second process of the heat exchange in the ultrasonic wave is realised in dispersions. It is associated with the heat flow between microscopic parts of dispersions, which thermophysical properties are different. This process and its effect on compressibility of liquids are discussed in the Section 3.

2.3 Inertial density of microemulsions

Deviation of the effective inertial density, ρ_I, of a dispersion from its gravimetric density (mass of unit of volume), ρ, is determined by the different accelerations of the dispersed particles and of the continuous medium, in a gradient of pressure in ultrasonic wave. For an oscillating gradient of pressure this difference is controlled by the ratio of the size if the particles to the wavelength of the shear wave, λ_η ($= \sqrt{\frac{4\pi\eta}{f\rho}}$, η is viscosity of the medium). The parameter $\frac{\lambda_\eta}{2\pi}$ (exponential decay length of the shear wave) determines the effective thickness of the transition layer around the border between the particle and the continuous medium, within which the speed of the medium changes from the speed at the border to the speed of the bulk medium. Dependence of λ_η on frequency (Figure 1 (a)) results in a change of the value of ρ_I from the value equal to the gravimetric density at low frequencies, to a different value at high frequencies (Povey, 1997).

The effect of frequency on ρ_I can be illustrated qualitatively by considering a rigid container filled with a liquid dispersion, and a periodic force applied to the walls of the container. The effective inertial mass of the container is the ratio of the applied force to the acceleration of the container. At low frequencies, when the transition layer around the borders between the particles and the continuous medium exceeds the size of the container, the speed and acceleration of the particles are the same for all parts of the container. In this case the effective inertial mass of the container is the sum of the masses of its parts (gravimetric mass): the particles, the continuous medium and the walls. At high frequencies, when the transition layer is smaller than the size of particles, the acceleration of the particles and the continuous medium are different. This results in a deviation of the effective inertial mass of the container from its gravimetric mass.

Microemulsions droplets normally are much smaller than the wavelength of the shear wave at ultrasonic frequencies (Figure 1 (a)). Also, the 'density contrast' determined by the difference between the density of the continuous medium and the droplets is relatively small. Therefore, for microemulsions $\rho_I = \rho$, which will be assumed below. If required, the outlined equations can be upgraded by including an appropriate relationship between ρ and ρ_I. In further discussions we will use the specific volume, v ($\equiv \frac{1}{\rho}$) and specific adiabatic compressibility,

k_S ($\equiv v\beta_S$) instead of the density and the coefficient of adiabatic compressibility, β_S, of medium. In this case the equation for ultrasonic velocity in liquids is transformed to:

$$u = \frac{v}{\sqrt{k_S}} \tag{4}$$

3. Compressibility of solutes and solute particles in liquid mixtures

3.1 Apparent compressibility of solutes

Contribution of solute to the compressibility, K_S, and the volume, V, of a mixture composed of the mass of solute m_{solute} and the mass of solvent m_0 can be characterised by the specific apparent adiabatic compressibility, φK_S, and the specific apparent volume, φV, of the solute:

$$\varphi K_S \equiv \frac{K_S - K_{S_0}}{m_{solute}}; \qquad \varphi V \equiv \frac{V - V_0}{m_{solute}} \tag{5}$$

Here and below the subscript indexes *solute* and 0 are referred to the properties of the solute and pure solvent. The above equations provide the relationships linking the specific volume and compressibility of the mixture and of the pure solvent with the apparent characteristics of solute:

$$\begin{aligned} v &= (1-w)v_0 + w\varphi V; & \varphi V &= \frac{v - v_0}{w} + v_0 \\ k_S &= (1-w)k_{S_0} + w\varphi K_S; & \varphi K_S &= \frac{k_S - k_{S_0}}{w} + k_{S_0} \end{aligned} \tag{6}$$

where w ($\equiv \frac{m_{solute}}{m_0 + m_{solute}}$) is the concentration (weight fraction) of the solute in the mixture. The Equations (6) are often used for calculations of φK_S and φV from the measured compressibility and volume (or density) of the mixture and of pure solvent.

The apparent properties represent the change of compressibility and volume of liquid caused by addition of solute to solvent. They can be measured experimentally and do not depend on the initial state of the solute (prior to its addition to solvent). However, in many cases they do not represent the state of the solute in the mixture due to solvation effects, which affect the state of the solvent. These effects include a transfer of components of solvent from the free (bulk) to the solvation state, which contributes to the measured apparent characteristics. In w/o microemulsions the solvation effects are represented by the transfer of surfactant (and cosurfactant) from the oil phase to the surface of microemulsion droplet, when water is added as a solute. Some amount of oil can also be incorporated into the solute particle (water pool surrounded by surfactant), especially between the hydrophobic tails of surfactant. Below we will apply the term 'solute particle' for particulates of solute, which are dispersed in the bulk solvent, and which may include some omponents of solvent. In case of solutions this term shall be applied to solvated solute molecules. To characterise the compressibility and the volume of the solute particle in its physical state in the mixture the specific apparent volume

and adiabatic compressibility of solute particle, v_{sp} and k_{sp}, can be introduced in the same way as the apparent characteristics of solute:

$$\begin{aligned} v_{sp} &\equiv \frac{V - V_{0sp}}{m_{sp}}\ ;\quad v = (1 - w_{sp})v_{0sp} + w_{sp}v_{sp};\qquad v_{sp} = \frac{v - v_{0sp}}{w_{sp}} + v_{0sp} \\ k_{S\,sp} &\equiv \frac{K_S - K_{S_0\,sp}}{m_{sp}};\quad k_S = (1 - w_{sp})k_{S_0\,sp} + w_{sp}k_{S\,sp};\quad k_{S\,sp} = \frac{k_S - k_{S_0\,sp}}{w_{sp}} + k_{S_0\,sp} \end{aligned} \tag{7}$$

where V and K_S are the volume and the adiabatic compressibility of the mixture containing the solvent and solute particles, m_{sp} ($\equiv m_{solute} + m_{solvent\,sp}$) is the mass of solute particles in the mixture, which includes the mass of the solvent incorporated into the solute particle, $m_{solvent\,sp}$, V_{0sp} and $K_{S_0\,sp}$ are the volume and the adiabatic compressibility of the bulk solvent in the mixture. In some cases the specific apparent volume and adiabatic compressibility of solute particles can be measured directly by adding all the components of solute particle to the solvent (measuring of v, v_{0sp}, k_S and $k_{S_0\,sp}$). They can also be calculated from the measured specific apparent volume and adiabatic compressibility of the solute as:

$$v_{sp} = \frac{\varphi V + w_s v_0 + \delta v_0 (1 + w_s - \frac{1}{w})}{(1 + w_s)};\ k_{S\,sp} = \frac{\varphi K_S + w_s k_{S_0} + \delta k_{S_0} (1 + w_s - \frac{1}{w})}{1 + w_s} \tag{8}$$

where w_s ($\equiv \frac{m_{solvent\,sp}}{m_{solute}}$, $m_{solvent\,sp}$ is the mass of solvent in the mixture incorporated into the solute particle) is the solvation level of the solute, δv_0 ($\equiv v_{0\,sp} - v_0$, $v_{0\,sp}$ is the specific volume of the bulk solvent in the mixture) is the difference between the specific volumes of the pure solvent and of the bulk solvent in the mixture and δk_{S_0} ($\equiv k_{S_0\,sp} - k_{S_0}$, $k_{S_0\,sp}$ is the specific adiabatic compressibility of the bulk solvent in the mixture) is the difference in between the specific adiabatic compressibilities of the pure solvent and of the bulk solvent in the mixture. Equation (8) is a consequence of Equations (6) and (7). The concentration of solute, w, in this equation reflects the dependence of δv_0 and δk_{S_0} on w at constant solvation level, w_s, when these values are not equal to 0. If solvation does not affect the composition of solvent the values of δv_0 and δk_{S_0} are equal to zero. In this case w vanishes from the above equation.

Similar to the above other apparent thermodynamic characteristics of solute and thermodynamic characteristics of solute particles can be introduced. This includes thermal expansibility, E ($\equiv \left(\frac{\partial V}{\partial T}\right)_P$), heat capacity, C_P ($\equiv \left(\frac{\partial H}{\partial T}\right)_P$, H is the enthalpy of the mixture), and isothermal compressibility, K_T ($\equiv -\left(\frac{\partial V}{\partial P}\right)_T$), thus producing the specific apparent thermal expansibility, φE, specific apparent heat capacity, φC_P, specific apparent isothermal compressibility, φK_T, specific isothermal compressibility of solute particle, $k_{T\,sp}$, specific thermal expansibility of solute particle, e_{sp}, and specific heat capacity of solute particle, $c_{P\,sp}$, of the solute particles defined as:

$$\varphi E = \frac{E - E_0}{m_{solute}};\quad \varphi C_P = \frac{C_P - C_{P_0}}{m_{solute}};\ \varphi K_T = \frac{K_T - K_{T_0}}{m_{solute}};\ e_{sp} = \frac{E - E_{0\,sp}}{m_{sp}};\ c_{P\,sp} = \frac{C_P - C_{P_0\,sp}}{m_{sp}};\ k_{T\,sp} = \frac{K_T - K_{T_0\,sp}}{m_{sp}}$$

where the abbreviations 0 and sp has the same meaning as above. Thus, the specific thermal expansibility, $e\ (\equiv \frac{E}{m})$, specific heat capacity, c_P and specific isothermal compressibility, $k_T\ (\equiv \frac{K_T}{m})$, of a mixture are presented as:

$$\begin{aligned} &e = (1-w)e_0 + w\varphi E;\ \ c_P = (1-w)c_{P_0} + w\varphi C_P;\ k_T = (1-w)k_{T_0} + w\varphi K_T \\ &e = (1-w_{sp})e_{0\,sp} + w_{sp}e_{sp};\ \ c_P = (1-w_{sp})c_{P_0\,sp} + w_{sp}c_{P\,sp};\ k_T = (1-w_{sp})k_{T_0\,sp} + w_{sp}k_{T\,sp} \end{aligned} \tag{9}$$

Parameters φK_S, φV, v_{sp} and k_{sp} characterise the state of the whole solute or the whole pool of solute particles in the mixture. If the state of the solute depends on its concentration it is often useful to interpret the data in terms of specific partial characteristics of solutes, $\bar{v}$ and $\bar{k}_S$, defined as a change of volume, V, or compressibility, K_S, of the mixture caused by addition of infinitely small mass of solute δm_{solute}:

$$\begin{aligned} \bar{v} &\equiv \left(\frac{\partial V}{\partial m_{solute}}\right)_{m_0} = \varphi V + w(1-w)\left(\frac{\partial(\varphi V)}{\partial w}\right)_{m_0};\\ \bar{k}_S &\equiv \left(\frac{\partial K_S}{\partial m_{solute}}\right)_{m_0} = \varphi K_S + w(1-w)\left(\frac{\partial(\varphi K_S)}{\partial w}\right)_{m_0} \end{aligned} \tag{10}$$

where the symbol m_0 represents constant amount of other (than solute) components of the mixture. The partial characteristics can be calculated from the measured apparent characteristics, φK_S and φV, and the slope of their concentration dependence, $\left(\frac{\partial(\varphi V)}{\partial w}\right)_{m_0}$ and $\left(\frac{\partial(\varphi K_S)}{\partial w}\right)_{m_0}$. In the same way the specific partial volume and compressibility of solute particles, $\bar{v}_{sp}$ and $\bar{k}_{S\,sp}$, can be introduced:

$$\begin{aligned} \bar{v}_{sp} &\equiv \left(\frac{\partial V}{\partial m_{sp}}\right)_{m_0\,sp} = v_{sp} + w_{sp}(1-w_{sp})\left(\frac{\partial v_{sp}}{\partial w}\right)_{m_0\,sp};\\ \bar{k}_{S\,sp} &\equiv \left(\frac{\partial K_S}{\partial m_{sp}}\right)_{m_0\,sp} = k_{S\,sp} + w_{sp}(1-w_{sp})\left(\frac{\partial k_{S\,sp}}{\partial w}\right)_{m_0\,sp} \end{aligned} \tag{11}$$

3.2 Thermal low and thermal high frequency limits for compressibility

Below we will consider mixtures of solute particles (molecules or molecular aggregates) surrounded by solvent. If the physical properties of the solute particles and the solvent are different, a change of pressure in the mixture results in a different change of the temperature

within the solute particles and within the surrounding solvent. This causes a heat flow between the particles and the solvent, which affects the volume change during compression. Thus, the effects of solute particle – solvent heat exchange shall be included in interpretations of measured compressibilities.

Two major structural characteristics control the change of the volume of the mixture when an excessive pressure is applied. The first is the length scale of homogeneity of pressure within the mixture, which is determined by the wavelength of the ultrasonic wave, λ. For the practical frequency range of precision measurements of compressibility, 1 to 100 MHz, λ is between 10^6nm and 10^4nm (Figure 1 (a)). Therefore for the nano-scale particles of the size below 1000 nm the effects of non-homogeneity of pressure around them can be neglected. The second structural characteristic, is the wavelength of the thermal wave, λ_T, (or the decay length, $\delta_T = \frac{\lambda_T}{2\pi}$), which determines the portions of the solute particle and the

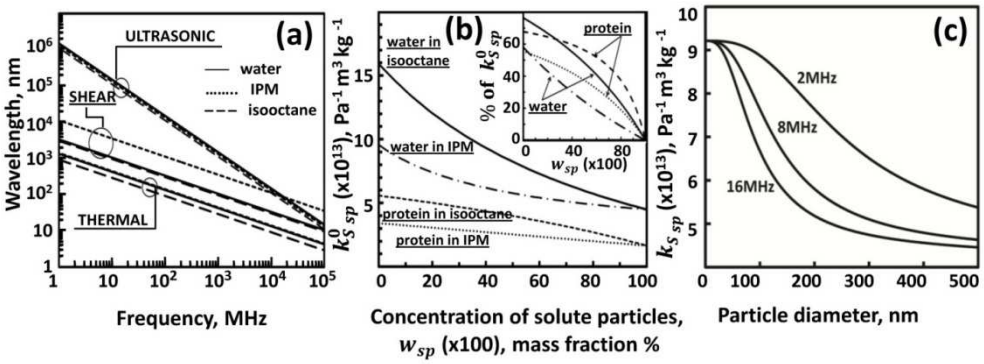

Fig. 1. (a): Wavelength as function of frequency for ultrasonic, λ, thermal, λ_T, and shear, λ_η waves in pure water, IPM system (composition described in Section 6) and in isooctane at 25°C calculated using physical parameters given in Table 1. (High GHz frequency part of the plot for illustrative purposes only as the physical properties of the media at high frequencies are expected to deviate from those at low frequencies). **(b): Main frame.** Specific adiabatic compressibility of protein particles and of droplets of water in IPM system and in isooctane at 25°C calculated for thermal low frequency limit using Equation (14) and physical properties given in Table 1. **Insert.** The 'solvent' part of adiabatic compressibility of protein particles and droplets of water in IPM and in isooctane as % of $k^0_{S\,sp}$ shown in the main frame; calculated using Equations (13) and (16). **(c):** Effect of droplet size on specific adiabatic compressibility of droplets of water in IPM system at different frequencies and at 25°C calculated as described in Section 3.4.

solvent involved in the heat exchange. In liquids λ_T varies between 100nm and 1000nm for the practical frequency range of precision measurements of compressibility, 1 to 100 MHz (Figure 1 (a)). This is within the range of the sizes of particles of dispersions, thus producing a profound effect of the frequency of ultrasound on the measured compressibility of the micro particles in mixtures. With respect to this, two limiting cases

can be distinguished. 1) At **thermal low frequency limit** the period of compression is much longer than the time required for the heat exchange within the compressed volume. Under this condition the complete thermal equilibrium within the compressed volume is achieved and all its parts have the same temperature at each time. 2) At **thermal high frequency limit** the period of compression is much shorter than the time required for the heat exchange between the solute particles and the bulk solvent. Under this condition the solute particles and the solvent are thermally insulated. In structural terms the thermal low frequency limit is realised when the size of the solute particles, l, is much smaller than the wavelength of the thermal wave, $l << \lambda_T$. For the thermal high frequency limit $l >> \lambda_T$. In this case the volume (and the thermal mass) of the transition layer around the border between the solute particle and the solvent, where the solute-solvent heat exchange takes place, is negligibly small when compared with the volume of the solute particles and the solvent. Therefore, compressibility of particles, polymers and molecular aggregates with the size about and below 10 nm shall be attributed to the thermal low-frequency limit, while compressibility of particles and aggregates with the size of microns and higher shall be described in terms of thermal high-frequency limit especially at the top of the frequency range. Below the uppercase symbol ^{0} will be used for variables at low frequency limit and $^\infty$ for high frequency limit. An absence of these symbols will presume general cases applicable for both limits, or their irrelevance.

3.3 Apparent compressibility of solutes and compressibility of solute particles at thermal low and thermal high frequency limits

At thermal low frequency limit all parts of the mixture are at the same temperature, and therefore, have the same value of $\frac{\delta T}{\delta P} = \frac{Te}{c_P}$. Thus, the specific adiabatic compressibility of the mixture at this limit, k_S^0, is given by: $k_S^0 = k_T - \frac{Te^2}{c_P}$ where e and c_P are specific thermal expansibility and heat capacity of the mixture given by Equation (9). This and Equations (6) and (7) provide the relationship for specific apparent adiabatic compressibility of solute at thermal low-frequency limit, $\varphi K_S{}^0$, and specific adiabatic compressibility of solute particle at this limit, $k_{S\,sp}^0$:

$$\varphi K_S^0 = \varphi K_T - \frac{e_0^2 T}{c_{P_0}}\left(2\frac{\varphi E}{e_0} - \frac{\varphi C_P}{c_{P_0}} + w\frac{\left(\frac{\varphi E}{e_0} - \frac{\varphi C_P}{c_{P_0}}\right)^2}{1 + w\left(\frac{\varphi C_P}{c_{P_0}} - 1\right)}\right)$$

$$k_{S\,sp}^0 = k_{T\,sp} - \frac{e_{0sp}^2 T}{c_{P_0\,sp}}\left(2\frac{e_{sp}}{e_{0\,sp}} - \frac{c_{P\,sp}}{c_{P_0\,sp}} + w_{sp}\frac{\left(\frac{e_{sp}}{e_{0\,sp}} - \frac{c_{P\,sp}}{c_{P_0\,sp}}\right)^2}{1 + w_{sp}\left(\frac{c_{P\,sp}}{c_{P_0\,sp}} - 1\right)}\right) \quad (12)$$

The above equations demonstrate that at thermal low frequency limit the specific apparent adiabatic compressibility of the solute and adiabatic compressibility of solute particles depend on the concentration even in ideal mixtures. The third terms of Equations (12)

represent a reduction of the solute–solvent heat exchange with concentrations, w and w_{sp}, due to the lowering of the amount of solvent in the mixture. At infinite dilution ($w, w_{sp} \to 0$) Equations (12) are reduced to:

$$\varphi K_S^0 = \varphi K_T - \frac{e_0^2 T}{c_{P_0}}\left(2\frac{\varphi E}{e_0} - \frac{\varphi C_P}{c_{P_0}}\right); \quad k_{S\,sp}^0 = k_{T\,sp} - \frac{e_{0sp}^2 T}{c_{P_0\,sp}}\left(2\frac{e_{sp}}{e_{0\,sp}} - \frac{c_{P\,sp}}{c_{P_0\,sp}}\right) \tag{13}$$

At thermal high frequency limit no heat exchange between solute particles and the surrounding solvent is present. Therefore, the compressions of solute particles and the solvent occur independently on each other, and the adiabatic compressibility of the mixture at this limit, K_S^∞, is an additive thermodynamic characteristic. Thus, the apparent specific adiabatic compressibility at thermal high frequency limit, φK_S^∞, in ideal mixture does not depend on concentration. At $w = 1$ the Equations (12) transform to $(\varphi K_S^0)_{w=1} = \varphi K_T - \frac{T\varphi E^2}{\varphi C_P}$ and at $w_{sp} = 1$ to $k_{S\,sp}^0 = k_{T\,sp} - \frac{T e_{sp}^2}{c_{P\,sp}}$. Also at $w = 1$ the heat exchange between the solute and the solvent vanishes and, therefore, compressions occur at adiabatic condition for the solute and at $w_s = 1$ for the solute particle at all frequencies. Therefore, $(\varphi K_S{}^0)_{w=1} = (\varphi K_S{}^\infty)_{w=1}$. As for ideal mixture of solute and solvent the value of φK_S^∞ does not depend on the concentration, the relationship $\varphi K_S^\infty = \varphi K_T - \frac{T(\varphi E)^2}{\varphi C_P}$ shall be valid for any concentration. It is important to note that this relationship is correct only for ideal mixture of solute and solvent. At $w_{sp} = 1$, $k_{S\,sp}^0$ represents the adiabatic compressibility of pure solute particle: $k_{S\,sp}^0 = k_{S\,sp}^\infty$. With respect to $k_{S\,sp}^0$ Equations (12) can be rewritten in the following form:

$$k_{S\,sp}^0 = k_{S\,sp}^\infty + k_{HE\,sp}; \qquad k_{S\,sp}^\infty = k_{T\,sp} - \frac{e_{sp}^2 T}{c_{P\,sp}}$$

$$k_{HE\,sp} = \underbrace{\frac{e_{0\,sp}{}^2 T}{c_{P_0\,sp}}\left(\frac{c_{P\,sp}}{c_{P_0\,sp}} - \frac{e_{sp}}{e_{0\,sp}}\right)^2 \frac{c_{P_0\,sp}}{c_{P\,sp}}}_{\text{Contribution of heat exchange between the solute particle and infinite amount of solvent}} - \underbrace{w_{sp}\frac{\frac{e_{0\,sp}{}^2 T}{c_{P_0\,sp}}\left(\frac{c_{P\,sp}}{c_{P_0\,sp}} - \frac{e_{sp}}{e_{0\,sp}}\right)^2}{1 + w_{sp}\left(\frac{c_{P\,sp}}{c_{P_0\,sp}} - 1\right)}}_{\text{Reduction of contribution of heat exchange caused by substitution of solvent with solute particles}} \tag{14}$$

where $k_{S\,sp}^\infty$ is the specific adiabatic compressibility of the solute particle at thermal high frequency limit and k_{HE} is the contribution of the heat exchange between the solute particle and its environment to compressibility. The specific adiabatic compressibility of solute particle at thermal high frequency limit, $k_{S\,sp}^\infty$, represents the 'true' adiabatic compressibility of the particle. In contrast to this, the specific adiabatic compressibility of solute particle measured at thermal low frequency limit has a contribution from the heat exchange between the solute particle and its environment and, therefore, depends on the properties of solvent

even in the absence of solvation effects. Figure 1 (b) represents the compressibility $k^0_{S\,sp}$ of globular protein and of droplets of water in two solvents, pure isooctane and in IPM system (composition is given in Table 1), calculated according to Equation (14). The physical properties of solute particles ($''_{sp}$) and bulk solvent ($''_{0\,sp}$) used in the calculations are given in Table 1. As no solvation effects were included in calculations ($w_s = 0$), the concentration w_{sp} represents the concentration of solute, $w_{sp} = w$. Figure 1 (b) shows that the compressibility of solute particles at thermal low frequency limit depends significantly on the properties of solvent. Aqueous mixtures, where water is the solvent, are different in this respect, when compared with others, due to the 'abnormal' physical characteristics of liquid water at room temperatures and below: very low value of thermal expansibility, $e_{0\,sp} << e_{sp}$, and high value of heat capacitance, $c_{P_0\,sp} >> c_{P\,sp}$. For aqueous mixtures $(\frac{c_{P\,sp}}{c_{P_0\,sp}} - \frac{e_{sp}}{e_{0\,sp}})^2 \approx (\frac{e_{sp}}{e_{0\,sp}})^2$ and, according to Equation (14), at low concentrations the adiabatic compressibility of solute particle at thermal low frequency limit, $k^0_{S\,sp}$, is close to its isothermal compressibility, $k_{T\,sp}$: $k^0_{S\,sp} \approx k^\infty_{S\,sp} + \frac{e_{sp}{}^2 T}{c_{P\,sp}} = k_{T\,sp}$.

Equations (12) or (14) can be applied for calculations of adiabatic compressibility of solute particle, or apparent compressibility of solute in a Solvent 2, $k^0_{S\,sp\,2}$ or φK^0_{S2} from the compressibility measured in a different solvent, Solvent 1, $k^0_{S\,sp\,1}$ or φK^0_{S1}. If the substitution of solvents does not affect the following additive characteristics of solute particles or solute, $k^\infty_{S\,sp}$ (or $k_{T\,sp}$), e_{sp}, $c_{P\,sp}$ or φK_T, φE, φC_P, for infinite dilution, $w \to 0$:

$$\varphi K^0_{S2} = \varphi K^0_{S1} + \frac{e^2_{01} T}{c_{P_0 1}}[2\frac{\varphi E}{e_{0\,1}}(1-R) - \frac{\varphi C_P}{c_{P_0 1}}(1-R^2)]; \quad where \;\; R \equiv \frac{e_{0\,2}\, c_{P_0 1}}{e_{0\,1}\, c_{P_0 2}}$$
$$k^0_{S\,2\,sp} = k^0_{S1\,sp} + \frac{e^2_{0\,1sp} T}{c_{P_0 1sp}}[2\frac{e_{sp}}{e_{0\,1sp}}(1-R_{sp}) - \frac{c_{P\,sp}}{c_{P_0\,sp\,1}}(1-R_{sp}{}^2)]; \; where \;\; R_{sp} \equiv \frac{e_{0\,2\,sp}\, c_{P_0 1sp}}{e_{0\,1sp} c_{P_0\,2\,sp}} \quad (15)$$

3.4 Transition between thermal low and thermal high frequency limits

As frequency increases the compressibility of solute particle changes from its value for thermal low frequency limit to the value at thermal high frequency limit in the frequency range for which λ_T is comparable with the size of solute. The analytical dependence of compressibility on the frequency for a given size of the solute or on the size of the solute for a given frequency can be obtained through analysis of dynamics of the heat exchange between the solute particles and the solvent. The results depend on structural details of the mixture including particle geometry. Algorithms of this analysis were described previously as a part of ultrasonic scattering theories (Isakovich, 1948; Hemar et al., 1998; Allegra & Hawley, 1972; Povey, 1997) although specific calculations normally were limited to the case of spherical particles. Certain aspects of the results can be generalised. An increase of the frequency decreases the volumes of the solute particle and the solvent participating in the heat exchange around the particle-solvent border. These volumes involve the whole particle and the solvent at low frequencies and become to be negligibly small at high frequencies. The dependence of compressibility on

lg of frequency (or on lg of size at constant frequency) exhibits an 'S' shape curve. The main transition of compressibility between the thermal low and thermal high frequency limits occurs around frequency at which the size of solute particle is about the wavelength of the thermal wave. The major change of compressibility with frequency occupies within one decade on the frequency range. Figure 1(c) demonstrates the dependence of compressibility of aqueous droplets on their particle size in the IPM system at $w_{sp} = 0.01$ calculated using the PSize software module (v.2.28.01) provided with HR-US 102 spectrometers (Sonas Technologies Ltd.). This software utilises theoretical approaches developed previously for spherical particles in liquid continuous medium (Epstein & Carhart, 1953; Waterman & Truell, 1961; Allegra & Hawley, 1972; Povey, 1997; Austin et al., 1996). The physical properties used in the calculations are given in Table 1. The calculated values of compressibility for zero and infinite diameter agree well with values of adiabatic compressibility for thermal low and thermal high frequency limits, calculated according to Equation (14). An exception to this is a very small deviation at zero limit of diameter of particle. This could be expected as the cited theories do not account well the concentration behaviour of the heat exchange between the particles and the solvent.

3.5 Molecular interpretation of compressibility of solute particles

Molecular interpretation of compressibility requires distinguishing contributions of different origin to compressibility. For an ideal mixture of solute particles and a solvent three major contributions shall be considered: intrinsic compressibility of solute particle, $k_{S\,in}$, ideal contribution to compressibility, $k_{S\,id}$, and relaxation contribution to compressibility, $k_{S\,rel}$. At infinite dilution $k_{S\,sp} = k_{S\,in} + k_{S\,id} + k_{S\,rel}$.

3.5.1 Ideal contribution to compressibility of solute particle

The ideal contribution to compressibility of solute particles represents compressibility of particles with zero intrinsic volume and intrinsic compressibility. It is originated by the heat motion of the solute particles, which produces an 'additional' (osmotic) pressure in the mixture, thus leading to the expansion of solvent. The change of the volume of this expansion with external pressure provides the ideal contribution to compressibility. Due to the origin (heat motion) of ideal compressibility, its molar value does not depend on the molar mass of solute particle, M. Therefore, its contribution to specific compressibility of solute particle is inversely proportional to molar mass, $k_{S\,id} \sim M^{-1}$, and shall vanish as the molar mass increases. Estimations of this contribution in microemulsion systems with typical thermodynamic parameters of oils, water and their mixtures with surfactants, show that for micelles and microdroplets this contribution is small and normally can be neglected.

3.5.2 Relaxation contribution to compressibility of solute particle

The relaxation (also for some systems called 'structural') contribution to the apparent compressibility and the compressibility of solute particles arises if the particles have different states (conformational, protonated, etc.) in the mixture, and the distribution between the states changes following changing pressure and temperature in ultrasonic wave. The relaxation contribution to compressibility represents the change of the volume of the mixture caused by a

shift in the distribution of solute particles between different states, per unit of pressure applied. The basic relationships between the molecular characteristics of relaxation processes and their contributions to ultrasonic parameters were described previously (see for example Kaatze et al., 2000). The theories cover the thermal low frequency limit at which solute and solvent have the same temperature at any time. They provide tools for estimation of relaxation contribution from known volume and enthalpy effects of the relaxation process and the equilibrium concentrations of its participants. The frequency dependence of the relaxation compressibility is determined by factor $\frac{1}{1+(2\pi f\tau)^2}$ (τ is the relaxation time of the process). This allows ultrasonic analysis of kinetics of chemical processes. The relaxation compressibility vanishes at high frequencies.

At thermal high frequency limit each solute particle is thermally insulated, thus, oscillations of temperature within the particles of different states and within the solvent are different. Therefore, at this limit relationships between the ultrasonic parameters and molecular characteristics of relaxation processes are complex and depend on the structural details of mixtures.

3.5.3 Intrinsic compressibility of solute particles

Intrinsic adiabatic compressibility of solute particle is the part of compressibility of solute particle associated with intrinsic properties of particles. At thermal high frequency limit it represents the adiabatic compressibility of the material of particles (solutes). For low molecular weight molecules it is determined by the change of Van der Waals radii of atoms and the length of covalent bonds caused by applied pressure. The magnitude of this compressibility can be estimated from compressibilities of relevant crystals. For organic molecules it is much smaller than other contributions to compressibility and normally can be neglected. (see for example Buckin, 1988). Intrinsic compressibility of molecular aggregates and compact polymers at thermal high frequency limit can be qualitatively distinguished by the type of volume changes caused by compression: (a) volume change caused by compression of interatomic contacts (Van der Waals contacts, hydrogen bonding, etc.) and (b) volume change caused by a structural/conformational transitions between the states of different volume (structural contribution). As conformational (structural) transitions normally involve coordinated movement of large number of atomic groups (polymers) or molecules (molecular aggregates) their relaxation time is much longer than the relaxation time for compression of interatomic contacts. This often allows another way to distinguish the (a) and (b) types of contributions to compressibility of molecular aggregates and compact polymers. At high frequencies when the period of oscillation of pressure is much shorter than the relaxation time for a particular conformational transition, this transition will be 'frozen' and its contribution to compressibility vanishes. By their nature the (b) types of contributions to intrinsic compressibility of solutes are the relaxation contributions. For pure liquids the structural contribution normally represents about 30% of their total compressibility (Litovitz & Davis, 1964). Liquid water is an exception as the structural contribution (at room temperature) is about 60% of its compressibility. This is explained by its highly aggregated structure resulted from high level of hydrogen bonding between molecules. The remaining 40% of compressibility is close to the compressibility of ice crystals, which represent type (a) of intrinsic compressibility (Litovitz & Davis, 1964)).

Therefore, hydration processes are often accompanied by a significant decrease of compressibility of water. At thermal low frequency limit the contribution of heat exchange is added to the intrinsic compressibility which is provided by Equations (12) to (14).

3.5.4 Physical location of compressibility of solute particle

Compressibility of solute particle is defined as the difference between the compressibility of the mixture (solute particles in the bulk solvent) and the bulk solvent. At thermal high frequency limit the particle and the bulk solvent are thermally insulated, and, in an absence of ideal and relaxation contributions, compressibility of solute particle represents the compression of the physical volume of solute particle per unit of pressure applied. At thermal low frequency limit, the solute – solvent heat exchange affects the temperature of the particle and the solvent and, therefore, their compressions. Thus, at this frequency limit a part of the measured compressibility of solute particle is physically located in the solvent. It represents the difference between the compression of the solvent in the mixture and the compression of the pure solvent (per unit of pressure applied). A question can be raised on the portions of compressions of solute particle and the solvent contributing to compressibility of solute particle. These portions can be obtained from the following considerations. The specific adiabatic compressibility of the bulk solvent is given as: $k_{S_0\,sp} = k_{T_0\,sp} - e_{0\,sp}\left(\frac{\partial T}{\partial P}\right)_S$. In pure bulk solvent (same composition as in the mixture) $\left(\frac{\partial T}{\partial P}\right)_S = \frac{Te_{0\,sp}}{c_{P_0\,sp}}$. In the mixture at thermal low frequency limit $\left(\frac{\partial T}{\partial P}\right)_S = \frac{Te}{c_P} = T\frac{(1-w_{sp})e_{0\,sp} + w_{sp}e_{sp}}{(1-w_{sp})c_{P_0\,sp} + w_{sp}c_{P\,sp}}$. The difference between the compressibility of the bulk solvent in the mixture and the pure bulk solvent calculated per unit of mass of solute particle provides the portion of compressibility of the solute particle located in the bulk solvent, $k_{S\,sp\,solvent} : k_{S\,sp\,solvent} = -e_{0\,sp}\left(\frac{Te}{c_P} - \frac{Te_{0\,sp}}{c_{P_0\,sp}}\right)$, which can be rewritten as:

$$k_{S\,sp\,solvent} = -(1-w_{sp})\frac{Te_{0\,sp}{}^2}{c_{P_0\,sp}}\frac{\frac{e_{sp}}{e_{0\,sp}} - \frac{c_{P\,sp}}{c_{P_0\,sp}}}{1 + w_{sp}\left(\frac{c_{P\,sp}}{c_{P_0\,sp}} - 1\right)} \tag{16}$$

It is interesting to note that the 'solvent' part of compressibility of solute particle can be positive or negative, depending on the ratios of thermal expansibility and heat capacity for the particles and the solvent. The insert in the Figure 1(b) illustrates the portion of the 'solvent' part of $k^0_{S\,sp}$ for protein and for droplets of water in isooctane and in IPM system calculated according to the Equations (14) and (16). The physical properties of solute particles ($''_{sp}$) and solvent ($''_{0sp}$) used in the calculations are given in Table 1. As no solvation effects were included in calculations ($w_s = 0$), the concentration w_{sp} represented the concentration of solute, $w_{sp} = w$. Figure 1(b) demonstrates that the 'solvent' part of

compressibility of protein particles and droplets of water in these solvents is significant and at low concentrations exceeds 50%.

4. Ultrasonic measurements of apparent and partial compressibilities

4.1 Concentration increment of ultrasonic velocity

Equations (4) and (6) allow calculations of apparent adiabatic compressibility of solutes from the measured values of ultrasonic velocity and density. However, for dilute mixtures, where the contribution of solutes to the specific compressibility and the volume of the mixture is much smaller than the contribution of solvent, this way of obtaining of φK_S (and k_{sp}) possesses a problem as it requires very precise measurements of ultrasonic velocity and density in exactly the same mixture and at the same temperature. This is also complicated by the high temperature dependence of ultrasonic velocity and density, which means that during the measurements of velocity and density the temperature must be controlled with high precision. In addition, precision of measurements of the absolute values of ultrasonic velocity and density normally does not exceed 10^{-5} of the absolute value. However, the change in velocity, δu, and density, can be measured much better (down to 10^{-7} of absolute velocity (Buckin & Smith, 1999; Buckin & O'Driscoll, 2002) and 10^{-6} of density). Therefore, calculations of apparent adiabatic compressibility from the contributions of solutes to ultrasonic velocity and to specific volume of the mixture are more precise. These contributions are obtained from the measured change of ultrasonic velocity, δu ($\equiv u - u_0$, where u and u_0 are the velocity in the mixture and in the solvent), and of specific volume, δv, caused by addition of the solute to the solvent.

The contribution of solute to ultrasonic velocity in the mixture can be represented by the concentration increments of ultrasonic velocity of solute, such as a_u or a_{u^2}, defined as:

$$a_u \equiv \frac{\frac{u}{u_0} - 1}{w} = \frac{\delta u}{w u_0}; \qquad a_{u^2} \equiv \frac{(\frac{u}{u_0})^2 - 1}{2w} = \frac{\delta u(2u_0 + \delta u)}{2w{u_0}^2} \tag{17}$$

The two concentration increments of ultrasonic velocity are linked with each other as:

$$a_{u^2} = a_u(1 + \frac{w a_u}{2}) \tag{18}$$

At infinite dilution, $w \to 0$, the increments become to be equal: $a_u = a_{u^2}$. If required, the ultrasonic velocity of liquid can be calculated from the known concentration increment of ultrasonic velocity as: $u = u_0(1 + w a_u)$ or $u = u_0\sqrt{1 + 2w a_{u^2}}$. When analysing the properties of solute particles the concentration increments for solute particle can be introduced, $a_{u\,sp}$ and $a_{u^2\,sp}$, which are defined in the same way as a_u and a_{u^2}:

$$a_{u\,sp} \equiv \frac{\frac{u}{u_{0sp}} - 1}{w_{sp}} = \frac{\delta u_{sp}}{w_{sp} u_{0\,sp}}; \qquad a_{u^2\,sp} \equiv \frac{(\frac{u}{u_{0\,sp}})^2 - 1}{2w_{sp}} = \frac{\delta u_{sp}(2u_{0sp} + \delta u_{sp})}{2w_{sp}{u_{0\,sp}}^2} \tag{19}$$

where $u_{0\,sp}$ is the ultrasonic velocity for the bulk solvent in the mixture and $\delta u_{sp} = u - u_{0\,sp}$. If the value of ultrasonic velocity in the bulk solvent is the same as in the pure solvent, $u_{0\,sp} = u_0$, the proportionality coefficient $\frac{w_{sp}}{w} = 1 + w_s$ allows recalculations of specific concentration increments of ultrasonic velocity: $a_{u\,sp} = \frac{a_u}{1+w_s}$; $a_{u^2\,sp} = \frac{a_{u^2}}{1+w_s}$.

The concentration increments of ultrasonic velocity characterise the state of the whole solute in the mixture. If the state of the solute depends on its concentration it is often useful to obtain the partial concentration increments of ultrasonic velocity, $\bar{a}_u$ and $\bar{a}_{u^2}$, which represent the effect of addition of a small portion of solute to a solutions at a particular concentration:

$$\bar{a}_u \equiv \left(\frac{\partial}{\partial w}(\frac{u}{u_0})\right)_{m_0} = a_u + w\left(\frac{\partial a_u}{\partial w}\right)_{m_0}; \quad \bar{a}_{u^2} \equiv \frac{1}{2}\left(\frac{\partial}{\partial w}(\frac{u}{u_0})^2\right)_{m_0} = a_{u^2} + w\left(\frac{\partial a_{u^2}}{\partial w}\right)_{m_0} \tag{20}$$

Partial concentration increments of solute particles are introduced in the same way.

4.2 Calculations of apparent adiabatic compressibilities from concentration increments of ultrasonic velocity

Combination of Equation (4), (6), and (19) provide the following relationship for calculations of specific apparent adiabatic compressibility of solute and the specific compressibility of solute particle in a liquid from the concentration increments of ultrasonic velocity and the specific apparent volume:

$$\begin{aligned} \varphi K_S &= k_{S_0}(2\frac{\varphi V}{v_0} - 2a_{u^2} - 1 + w\frac{(\frac{\varphi V}{v_0} - 2a_{u^2} - 1)^2}{1 + 2wa_{u^2}}) \\ k_{S\,sp} &= k_{S_0\,sp}(2\frac{v_{sp}}{v_{0\,sp}} - 2a_{u^2\,sp} - 1 + w_{sp}\frac{(\frac{v_{sp}}{v_{0\,sp}} - 2a_{u^2\,sp} - 1)^2}{1 + 2w_{sp}a_{u^2\,sp}}) \end{aligned} \tag{21}$$

If the mixture contains gel structures, the contribution $\frac{M'_{gel}}{2w\rho u_0^2}$ shall be subtracted from a_{u^2} or $\frac{M'_{gel}}{2w\rho u_{0\,sp}^2}$ from $a_{u^2\,sp}$ (Equations (3), (17) and (19)) before applying Equations (21) for calculation of φK_S or $k_{S\,sp}$.

At infinite dilution, $w \to 0$, the Equations (21) are reduced to:

$$\varphi K_S = k_{S_0}(2\frac{\varphi V}{v_0} - 2a_u - 1); \qquad k_{S\,sp} = k_{S_0\,sp}(2\frac{v_{sp}}{v_{0\,sp}} - 2a_{u\,sp} - 1) \tag{22}$$

Equations (21) and (22) allow calculations of the specific apparent adiabatic compressibility of solutes and the specific adiabatic compressibility of solute particles from the measured concentration increment of ultrasonic velocity and apparent specific volume of solutes. When comparing the ultrasonic data with predictions of different models is often more practical to perform the analysis of directly measured concentration increment of ultrasonic velocity rather than of apparent adiabatic compressibility, thus excluding the need of the measurements of apparent volume. For this case Equations (21) can be rewritten in the following way, which allows calculations of concentration increment of ultrasonic velocity (as well as the ultrasonic velocity) from the specific apparent volume and compressibility of solute or the specific apparent volume and compressibility of solute particles:

$$a_{u^2} = \frac{1}{2}\left(2\frac{\varphi V}{v_0} - \frac{\varphi K_S}{k_{S_0}} - 1 + w\frac{\left(\frac{\varphi V}{v_0} - \frac{\varphi K_S}{k_{S_0}}\right)^2}{1 + w\left(\frac{\varphi K_S}{k_{S_0}} - 1\right)}\right);$$

$$a_{u^2\,sp} = \frac{1}{2}\left(2\frac{v_{sp}}{v_{0\,sp}} - \frac{k_{S\,sp}}{k_{S_0\,sp}} - 1 + w_{sp}\frac{\left(\frac{v_{sp}}{v_{0\,sp}} - \frac{k_{S\,sp}}{k_{S_0\,sp}}\right)^2}{1 + w_{sp}\left(\frac{k_{S\,sp}}{k_{S_0\,sp}} - 1\right)}\right) \tag{23}$$

At infinite dilution, $w \to 0$:

$$a_{u^2} = a_u = \frac{1}{2}\left(2\frac{\varphi V}{v_0} - \frac{\varphi K_S}{k_{S_0}} - 1\right); \qquad a_{u^2\,sp} = a_{u\,sp} = \frac{1}{2}\left(2\frac{v_{sp}}{v_{0\,sp}} - \frac{k_{S\,sp}}{k_{S_0\,sp}} - 1\right) \tag{24}$$

It is important to note that equations (21) to (24) are valid for the inertial low frequency limit only at which the inertial and gravimetric densities of the mixture are the same.

Equations (15) and (24) can be applied for calculations of a_u and $a_{u\,sp}$ at thermal low frequency limit and at infinite dilution in a Solvent 2, $a_{u\,2}$, from the value of a_u measured in a different solvent, Solvent 1, $a_{u\,1}$, provided that the substitution of solvents does not affect the followingcharacteristics of solute particles or solute, φK_T, φE, φC_P or $k_{S\,sp}^{\infty}$ ($k_{T\,sp}$), e_{sp}, $c_{P\,sp}$:

$$a_{u\,2} = a_{u1} R_k + \frac{\varphi V}{v_{0\,1}}(R_v - R_k) + TR_h\left[\frac{\varphi E}{e_{0\,1}}(1-R) - \frac{1}{2}\frac{\varphi C_P}{c_{P_0\,1}}(1-R^2)\right] - \frac{1}{2}(1-R_k)$$

$$a_{u\,2\,sp} = a_{u1\,sp} R_{k\,sp} + \frac{v_{sp}}{v_{0\,1\,sp}}(R_{v\,sp} - R_{k\,sp}) + TR_{h\,sp}\left[\frac{e_{sp}}{e_{0\,1\,sp}}(1-R_{sp}) - \frac{1}{2}\frac{c_{P\,sp}}{c_{P_0\,1\,sp}}(1-R_{sp}{}^2)\right] - \frac{1}{2}(1-R_{k\,sp}) \tag{25}$$

where $R_v \equiv \frac{v_{0\,1}}{v_{0\,2}}$, $R_k \equiv \frac{k_{S_0\,1}}{k_{S_0\,2}}$, $R_h \equiv \frac{R_k e_{0\,1}^2}{k_{S_0\,1}\, c_{P_0\,1}}$, $R_{v\,sp} \equiv \frac{v_{0\,1\,sp}}{v_{0\,2\,sp}}$, $R_{k\,sp} \equiv \frac{k_{S_0\,1\,sp}}{k_{S_0\,2\,sp}}$ and $R_{h\,sp} \equiv \frac{R_k e_{0\,1\,sp}^2}{k_{S_0\,1\,sp}\, c_{P_0\,1\,sp}}$.

5. Ultrasonic attenuation and particle sizing

Ultrasonic attenuation in emulsions, α, is represented by contributions of two terms: intrinsic absorption, α_I, and scattering losses, α_S: $\alpha = \alpha_I + \alpha_S$ (Povey, 1997)). For ideal mixture of solute particles and a solvent the intrinsic absorption is a sum of attenuations in the solvent, α_{I0}, and in the solute particle, α_{Isp}, weighted according to their volume fractions: $\alpha = \alpha_{I0}(1-x) + \alpha_{Isp}x + \alpha_S$ (x is the volume fraction of solute particles). The scattering contribution to ultrasonic attenuation, α_S, is a function of frequency, particle size and concentration, which is described by ultrasonic scattering theories. In the long wavelength limit, i.e. when the wavelength of ultrasound is much longer than the particle diameter, explicit expressions for the ultrasonic scattering in dispersions of spherical particles have been derived (Epstein & Carhart; 1953, Waterman & Truell, 1961; Allegra & Hawley, 1972; Povey, 1997). The mechanism of interaction of the ultrasonic wave with particles in dispersions in this regime contains two major contributors, thermoelastic and viscoinertial scattering. These contributions result from the 'scattering' of the incident ultrasonic waves into the thermal and the viscous waves propagating from the border between the particle and the continuous medium. The thermoelastic mechanism dominates in emulsions as the difference in density between the continuous and the dispersed phases of emulsions, which determines the magnitude of viscoelastic scattering, is not significant (Powey, 1997). Applications of ultrasonic scattering theories allow calculations of sizes of dispersed particles from the measured values of attenuation and the physical parameters of the continuous medium and the particles. The obtained sizes in microemulsions are in good agreement with the results of other techniques (Hickey et al., 2006, 2010).

6. Materials and methods

Materials. Ethyl oleate (Cat no. 27,074-1), sorbitan mono-laurate (Span 20, Cat no. 1338-39-2), polyoxyethylene 20 sorbitan mono-oleate (Tween 80, Cat no. 9005-65-6), isopropyl myristate (IPM) (cat. no. 110-27-0), n-propanol (cat. no. 71-23-8), doctyl sulfosuccinate sodium salt 98% (AOT) (cat no.577-11-7, lot# STBC 0203V) and 2,2,4-trimethylpentane (isooctane) 99.0% (cat no.540-84-1, lot# 53196MMV) were purchased from Sigma-Aldrich Chemical Co. Ltd. (Dublin, Ireland). Epikuron 200 (E200; soy lecithin, minimum 95 wt.% phosphatidylcholine; fatty acid content: palmitic and stearic, 16-20%; oleic acid, 8-12%; linoleic acid, 62-66%; linolenic acid, 6-8%, was supplied by Lucas Meyer (Germany). All reagents were of the highest purity available and were used as received. The ultrapure water (Millipore Super-Q-System) with the conductivity of 18.2 MΩ · cm^{-1} was used in sample preparation. Details of preparations of emulsions were described previously (Hickey et al., 2006, Hickey et al., 2010).

Microemulsion systems for ultrasonic titrations. **IPM**: isopropyl myristate & [Epikuron 200 : n-propanol (1:1, w/w)]; ratio of oil (isopropyl myristate) to surfactant+cosurfactant (Epikuron 200 + n-propanol (1:1, w/w)) was 60:40 (w/w). **EO**: ethyl oleate & [Tween 80:Span 20 (3:2, w/w)]; ratio of oil (ethyl oleate) to surfactant (Tween 80:Span 20 (3:2, w/w)) was 80:20 (w/w). **AOT**: 0.1M of AOT in isooctane.

Samples for enzyme reactions. D-cellobiose (purity ≥98%, Sigma-Aldrich Corp., Lot. 077K0741) was used for preparation of substrate samples for enzyme reaction. Aqueous solutions of D-cellobiose were prepared as 2.5% (w/w) of D-cellobiose in 10 mM sodium acetate buffer, pH 4.90. Substrate sample of D-cellobiose in microemulsion was prepared by mixing of 2.5

%(w/w) aqueous solution of D-cellobiose and IPM & [Epikuron 200 : n-propanol (1:1, w/w)] giving the following composition of microemuslion: IPM -38% (w/w); [Epikuron 200 : n-propanol (1:1, w/w)] - 38% (w/w); -water – 24% (w/w). Enzyme concentrations were determined by weight as a mass of liquid preparation (Novozyme 188 L (Novo Nordisk A/S); β-glucosidase preparation was obtained from *Aspergillus niger* microorganisms, with a declared minimum activity of 250 CbU per gram of liquid). Amount of protein in the preparation and other details of its composition were described earlier (Resa & Buckin, 2011). Enzyme was added to the substrate (cellobiose) solution (or emulsion) at room temperature and thoroughly mixed for 30 s, then degassed and loaded into the measuring cell of HR-US 102 differential ultrasonic spectrometer (Sonas Technologies Lt.) equilibrated at 25.0°C. The concentration of enzyme preparation in aqueous phase was 0.87 mg/mL. Ultrasonic measurements started immediately after loading (3 min after addition of enzyme to the substrate). Control experiments were performed by adding enzyme to same microemulsion and to the aqueous solution, however, without substrate to verify the stability of ultrasonic parameters within the time interval corresponding to the reaction time.

Titration profiles for ultrasonic velocity and attenuation in microemulsions were measured within 2 to 12 MHz frequency range at 25.0°C using a HR-US 102 SS (IPM, EO, AOT systems) and HR-US 102 (AOT system) differential ultrasonic spectrometers (Sonas Technologies Ltd.). The measuring ultrasonic cell (1.5 mL) was closed with a stopper, which incorporated a line for injection of titrant, drainage line for release of excess of sample and a mechanical mini stirrer. Measuring cell was fully filled with a mixture of oil, surfactant (and cosurfactant) using a calibrated Hamilton syringe. The exact amount of the mixture in the cell was determined by weighing the syringe before and after filling. Hamilton PB600 dispenser with 100uL Hamilton syringe attached to the injection line was used for the titrations. To exclude any possible evaporation the end of the drainage line was immersed in the enclosed vial filled with the mixture. The reference cell was filled with the same amount of the mixture and sealed. Measurements were continuously performed while the sample in the measuring cell was titrated with aliquots of degassed water. The stirring was activated after each addition of water and continued until no further change in the ultrasonic velocity and attenuation occurred, indicating that equilibrium had been reached. Following this stirring was stopped, stability of the measured values and attenuation was confirmed (5 to 10 minutes without stirring approximately) and next portion of water was added. *Density* was measured using Anton Paar 4500 density meter at 25.0°C connected with two flexible pipes to a 2 ml vial with a stirring bar inside filled with the mixture of oil and surfactant (and cosurfactant). Water was added stepwise to the vial in the same way as for ultrasonic measurements. After each addition several cycles of stirring and pumping of the mixture through the measuring cell were performed and stability of density readings were confirmed.

7. Ultrasonic phase diagrams

The ultrasonic phase diagrams can be obtained from titration profiles of ultrasonic velocity and attenuation. Simultaneous measurements of ultrasonic characteristics at various frequencies allow evaluation of their frequency dependence at each titration point. Overall, the titration profiles provide a number of parameters reflecting different levels of microstructural organisation of the system. In most cases transitions between different states of the system are clearly identified by an abrupt change of concentration profile of ultrasonic velocity,

attenuation and their frequency dependence. Figure 2 shows the ultrasonic titration profiles measured in three w/o microemulsion systems, IPM, AOT and EO, (described in Section 6) by stepwise additions of water into the mixture of oil & surfactant in the measuring cell of HR-US 102 spectrometer. The IPM and EO systems were studied by us previously (Hickey et al., 2006, 2010), however here we present new data on detailed titration profiles at low concentrations of water. Also, our new titration setup provided higher resolution of measurements. The concentrations of water corresponding to the same transitions for titrations at different oil:surfactant ratios provide the transition lines at ultrasonic pseudo-ternary phase diagrams. The positions of the transitions between the major phases such as microemulsion, coarse emulsion, liquid crystals, biocontinous on the ultrasonic phase diagrams agree well with the phase diagrams produced by other techniques for the above systems (Hickey et al., 2006, 2010). In addition to this, a range of transitions within the microemulsion phase were observed, which allowed upgrading the phase diagrams with additional 'sub phases' within the microemulsion phase. The nature of these 'sub phases' can be related to the state of water and surfactant, including hydration water in dispersed phase, hydration water in swollen reverse micelles and water in aqueous droplets surrounded by surfactant. Although, the details of these interpretations can be further discussed, it is important to recognize that ultrasonic technique allows the identification of these different 'sub-states' on the phase diagram in simple titration measurements. Consideration of these states and their position on the phase diagram is important in design of w/o microemulsions designated for encapsulation of active ingredients (e.g. proteins) functioning of which requires an appropriate level of their hydration. An example of this is discussed in the following chapters.

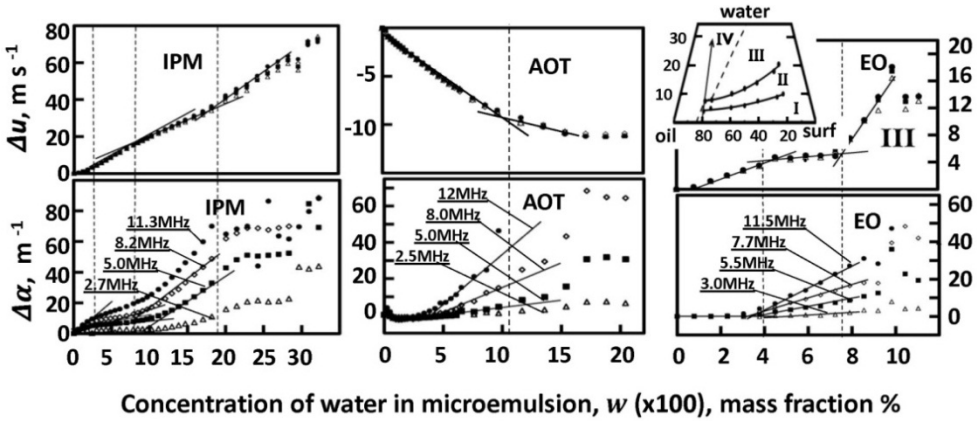

Fig. 2. Change of ultrasonic velocity and attenuation with concentration of water at 25°C in IPM, AOT and EO systems (see Section 6 for composition). The **insert** (EO system) represents the microemulsion part of ultrasonic phase diagram for EO system. The solid line with the arrow bar represents the ultrasonic titration line shown in in the main frame (EO). The points represent positions of the same transitions on ultrasonic titration lines for different oil:surfactant ratios. Transition between phases II and III is accompanied by appearance of UV/VIS light scattering. The dashed line ('- -') represents the data of (Alany et al., 2001) for transition between phases III and IV. I - hydration of surfactant with addition of water; II - formation of microemulsion droplets with a compact pool of water molecules; III - liquid crystals; IV - pseudobicontinuous phase.

In the IPM, AO and EO systems the end of microemulsion phase occurs at concentration of water of about 19%, 10% and 7.5%. Above these concentrations the microemulsions become to be opaque. This transition is marked by the appearance of a dispersion of ultrasonic velocity and abrupt change in the concentration slopes of attenuation and velocity. In addition to this, visible changes in the concentration profile (slope) of ultrasonic velocity and attenuation are observed within the concentration range of the microemulsion phase. For example, in IPM system the attenuation profile shows an initial increase up to the concentration 2%, than attenuation levels off between 2% and 8% approximately (exact concentration depends on the frequency), and begins to rise between 8% and 10% , with a linear part of the rise between 16% and 19%. Same pattern for transitions were observed for other titration lines, however at different concentrations of water. This could be interpreted as an existence of 'sub phases' within the microemulsion phase on the ultrasonic phase diagram, which are realised at concentrations of components between the transition lines. In AOT system the attenuation initially decreases to the concentration about 1.25%, or five molecules of water per one molecule of surfactant. This corresponds to the primary level of surfactant hydration (Spehr, 2010), which shall affect the intrinsic (relaxation) attenuation in the mixture of AOT and isopropanol. At concentrations above 2%, attenuation begins rising, which agrees with formation of droplets with a compact pool of water molecules described earlier (Hasegawa et al., 1994; Vasquez et al., 2011).

Several transition concentrations are also observed on velocity and attenuation profiles of EO system (Figure 2 EO). Formation of microemulsion droplets with a compact pool of water molecules in all systems can be attributed to the concentration points corresponding to a significant rise of ultrasonic attenuation: above 10% in IPM systems, above 2% in AOT system and 4 % for EO system. The amplitudes of this rise of attenuation and their frequency dependence correspond to the nanoscale (up to 20 nm for different parts of phase diagram) sizes of the water pool when ultrasonic scattering theories are applied (Hickey et al., 2006, 2010). This is in agreement with the absence of dispersion (dependence of frequency) of ultrasonic velocity (and compressibility) in the microemulsion part of the phase diagram, thus supporting the thermal low frequency conditions for microemulsion droplets. This is also in agreement with the results of light scattering and other techniques (Hickey et al., 2006, 2010; Hasegawa et al., 1994; Vasquez et al., 2011). The insert in Figure (2) shows the microemulsion part of the ultrasonic phase diagram for the EO system where the phase II corresponds to the existence microemulsion droplets with a compact pool of water molecules.

8. Compressibility of water in microemulsion droplets

The state of water in microemulsion droplets can be characterised by the apparent characteristics of water in microemulsion. As discussed above, the apparent adiabatic compressibility of water at a particular concentration represents the compressibility effect of addition of water to a mixture of oil and surfactant (and cosurfactant) and, therefore, is a sum of contributions of different states of water (water hydrating different atomic groups of surfactant/cosurfactant, 'free' water, if exists), and also contributions of compressibility effect of transferring of surfactant (cosurfactant) from oil to reversed micelles or to the exterior of the droplets of water at higher concentration of water. Therefore, it is also practical to consider the partial adiabatic compressibility of water,

which represents the effect of addition of a small amount of water to microemulsion at a particular concentration, and therefore, at a particular microscopic state of microemulsion system. If this addition is not accompanied by a restructuring of microemulsion, it shall reflect the compressibility of water in the state, adopted by the added molecules of water at the particular concentrations of components of microemulsion. If this state is 'free' water in microemulsion droplets, e.g. the properties of water are close to or the same as of the pure water, the specific compressibility of water shall be close to the compressibility of solute particles of 'free' water added to the microemulsion. The same shall be correct for the other partial characteristics of water such as partial volume or partial concentration increment of ultrasonic velocity (Hickey et al., 2006). However, obtaining the partial compressibility of solute as a slope of compressibility vs. concentration is accompanied with higher experimental errors, when compared with apparent compressibility. Thus, the requirements of high precision of ultrasonic measurements are of special importance in this case.

Figure 3 represents the experimental results for apparent and partial compressibilities of water in three microemulsion systems, IPM, EO and AOT, plotted for microemulsion part of the phase diagram. In this part no frequency dependence of compressibility was noticed for IPM, AOT and EO systems in the covered frequency range, 2 to 12MHz. In addition, the apparent and partial compressibility of aqueous solute particles in ideal mixture with oil and surfactant calculated at thermal low frequency limit (Equations (11) and (14)) are also plotted in the Figure 3. The required physical properties of water and the oil/surfactant (and cosurfactant) mixtures are given in the Table 1. Specific apparent volume and specific concentration increment of ultrasonic velocity, a_u, are also given in the Figure together with their partial characteristics and with characteristics of ideal solute particles (Equations (14), (20) and (23)) of pure water in the emulsion are also presented in the Figures. For the plotted range of concentrations the two increments of ultrasonic velocity, a_u and a_{u^2}, are practically coincide with each other. The data for φV in AOT microemulsion were taken from previous publications (Amararene et al, 1997). The slope of φK_{S_0} and a_u vs. concentration, required for partial characteristics, was taken as a 3 point average on the concentration dependence of φK_{S_0} and a_u.

As can be seen from the Figure 3 at low concentrations of water in microemulsion the apparent compressibilities and volumes and the partial compressibilities and volumes of water in all three microemulsion systems deviate significantly from the values calculated for ideal solute particles ('free' water). This shall be expected as an addition of water at low concentrations is accompanied by hydration of hydrophilic atomic groups of surfactant and co-surfactant and also by restructuring of surfactant aggregates in the mixture. As discussed above, the hydration effects for hydrophilic and charged atomic groups normally produce a significant reduction of compressibility of water. The difference between the measured characteristics of water in the microemulsions and the characteristics expected for ideal droplets of 'free' water decreases with concentration of water, especially in the part of the phase diagram, where a compact pool of water molecules exists. However in all three systems the measured partial compressibilities do not reach the level expected for the droplets of pure water. This indicates that the state of water in the droplets may be different to the state of free water. Some restructuring of surfactant at the water-oil interface, caused by its expanding with concentration of water may also contribute to the difference.

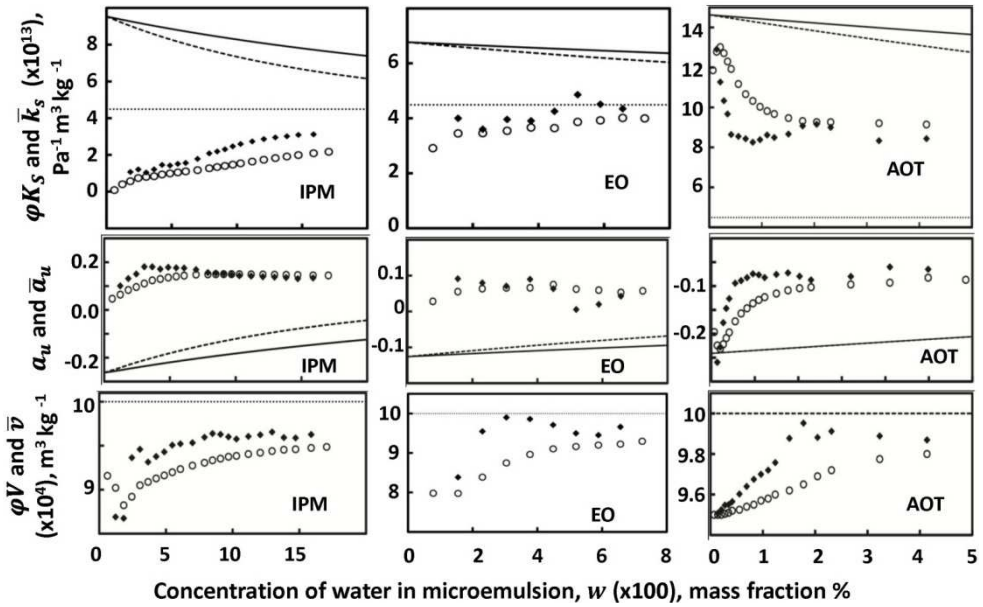

Fig. 3. Apparent (○), and partial (♦) characteristics of water at 25^{0}C in microemulsion part of phase diagrams for three w/o microemulsion systems (described in Section 6): IPM, EO and AOT (data for apparent and partial volume in AOT are taken from Amararene et al., 1997). The continuous ('-') and the dashed ('- -') lines represent the specific and the partial properties of droplets of pure water in microemulsion at thermal low frequency limit calculated according to Equations (14), (11), (23) and (20). The physical properties for these calculations are given in Table 1. The dotted lines ('···') represent the characteristics of pure water.

9. Effects of encapsulation on compressibility of globular proteins

Measurements of compressibility are often applied for characterisation of the state of solute particles in various environments and conditions. This includes characterisation of the state of solutes encapsulated in microemulsion droplets. The state of encapsulated proteins is of particular importance due to the growing interest to applications of microemulsions in various protein related technologies (bio-catalysis, protein extraction etc.). Compressibility of globular proteins, encapsulated on in w/o microemulsions, was studied previously in details (Valdez et al., 2001) for 0.1M AOT isopropanol microemulsion. The measurements were performed at one frequency, 10MHz. Figure 4(a) represents the apparent compressibilities encapsulated in AOT microemulsion for several globular proteins (Valdez et al., 2001) plotted by us as function of weight fraction of water in micoemulsion. The densities of microemulsions required for this plot were calculated using specific apparent volumes of water in 0.1M AOT w/o microemulsions published previously (Yoshimura et al., 2000; Amararene et al., 1997). Figure 4(a) shows that in microemulsion at low water content the apparent adiabatic compressibility of proteins is much higher than the compressibility of proteins in pure water. The increase of concentration of water decreases the apparent compressibility, which approaches the value for pure water at concentration of

water above 0.1 (w/w). The high value of the measured apparent adiabatic compressibility of proteins at low water content and its decrease with concentration of water is predicted by the Equations (12) or (14). The contribution of heat exchange to the compressibility of solute particle, $k_{sp\,HE}$, for isooctane solvent is significantly higher than for water. Addition of water to microemulsion reduces the portion of isooctane in the mixture, thus reducing the value of $k_{sp\,HE}$. If the size of microdroplets of water corresponds to the thermal low frequency conditions (all parts of the mixture are at the same temperature at any time of compression period), this substitution shall result in the proportional to the concentration of water, w_{water}, effect on the specific thermal expansibility, $e_{0\,sp}$ and specific heat capacity, $c_{P_0\,sp}$, of the environment of the protein globular:

$$e_{0\,sp} = e_{isooct}(1 - w_{water}) + e_{water} w_{water}; \quad c_{P_0\,sp} = c_{P_0\,isooct}(1 - w_{water}) + c_{P\,water} w_{water},$$

where indexes '*isooct*' and '*water*' mark the corresponding value for isooctane (with 0.1M AOT) and for water. Using these parameters for $e_{0\,sp}$ and $c_{P_0\,sp}$ in Equation (14) we have calculated the compressibility of solute particle having physical properties of globular protein (Table 1) as function of concentration of water in microemulsion, w_{water}. The calculations were performed for infinite dilution of protein ($w_{sp} = 0$), which corresponds to concentrations used in the measurements (Valdez et al., 2001) when concentration dependence of $k^0_{S\,sp}$ is considered (Figure 1(b) or Equation (14)). The dotted line in the Figure 4(a) represents the difference between the values of $k^0_{S\,sp}$ for protein at a particular concentration of water and the value in pure water ($w_{water} = 1$). The values of e_{water} and $c_{P_0\,water}$ were taken as characteristics of pure water, which is not absolutely correct as at least part of the water in the droplets is involved in hydration of polar groups of AOT and its physical properties may deviate from the physical properties of the bulk water. However, these parameters do not affect the limiting value of $k_{HE\,sp}$ at $w_{water} = 0$ and $w_{water} = 1$, as well as the general shape of its dependence on concentration of water. According to Figure 4(a) the above calculations predict reasonably well the apparent compressibility of the encapsulated globular proteins at zero concentration of water, as well as the observed decrease of compressibility with concentration of water. However, the exact functional dependence of the apparent compressibility on the concentration of water is different to the experimental one.

One of the possible explanations of lower than expected compressibility of encapsulated protein could be an effect of confine environment on the mechanical properties of protein globule, which can restrict the mobility of protein segments, thus making it more rigid (F. N. Kolisis & Stamatis, 2010). This will reduce the values of $k_{T\,sp}$ and $k_{S\,sp}$ in Equations (12) and (14) therefore the total compressibility of protein measured in microemulsion, $k_{S\,sp}$.

Another possible explanation can be presented when the structure of microdroplet of water containing a protein molecule is considered. Figure 4(a) shows that the drop of the measured compressibility occurs at much lower than predicted concentrations of water. This indicates that some amount of isooctane could be excluded from thermal exchange with the protein globules. This could be expected when the structure of microemulsion and the physical properties of isooctane are examined. The skin depth, δ_T, for isooctane is shorter than for other common solvents and at 10MHz is about 45 nm. This is comparable with the

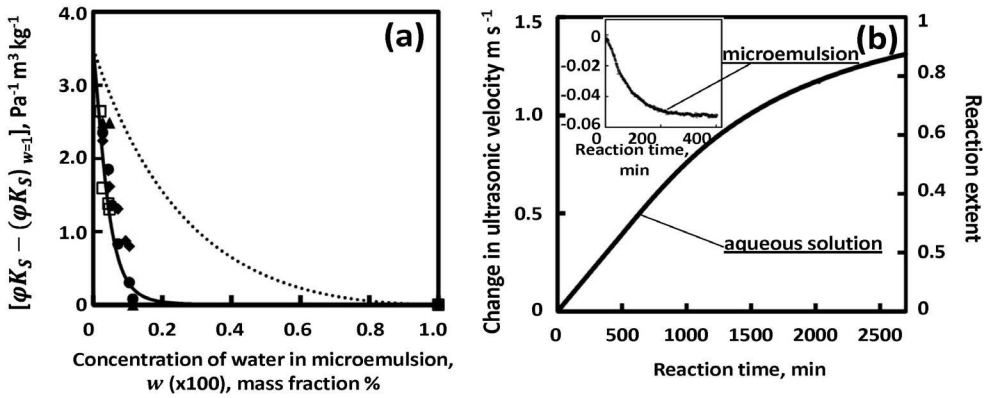

Fig. 4. **(a)**: Effect of concentration of water on specific apparent adiabatic compressibility of proteins (cytochrome c (□), MBP(▲), beta–lactoglobulin (○), lysozyme (♦)) encapsulated in AOT microemulsion. Compressibilities of proteins at 100% of water were subtracted. The lines represent predictions described in Chapter 9. **(b)**: Ultrasonic velocity time profile for hydrolysis of cellobiose by beta-glucosidase in aqueous solution (main chart) and in IPM microemulsion (50:50 w/w ratio of oil to surfactant + cosurfactant) at 25°C as described in Chapter 10.

size of droplets of water formed in 0.1M AOT isooctane microemulsion without protein, 5nm at concentration 0.075 (30 molecules of water per one molecule of surfactant) and larger at higher concentrations of water (van Dijk et al., 1989; Amararene et al., 2000). We could expect that a presence of protein molecules increases the size of the droplets. Thus, the conditions for thermal low frequency limit may not be held for this multilayer system (protein surrounded by water, surrounded by AOT and isooctane). In this case only a part of isopropanol in the mixture will be involved in the heat exchange with the protein globular thus increasing the 'effective' concentration (w/w) of water within the heat exchange volume. The accurate estimations of the effect of the heat exchange on the compressibility of the protein in this multilayer system can be done only when considering dynamics of heat exchange in a course of periodic compression within this system, which is outside of the scope of this paper. However, simplified modelling can be made to relate the effects of the heat exchange with the measured compressibility of proteins in AOT microemulsion. We can suggest that the environment of the protein globule, involved in the heat exchange, is a layer of water around protein with the thickness $r - r_p$ (r is the radius of the droplet and r_p is the radius of molecule of protein) and the layer of isooctane and surfactant of 'effective' thickness δ. The value of δ can be introduced as a thickness of solvent around the droplet which provides same as measured compressibility of protein particle if: (1) the volume comprised of the protein + water + δ layer of solvent is adiabatically insulated from the rest of the mixture and (2) a complete heat exchange between its parts occurs (same temperature for protein water and δ layer of solvent) during the course of compression. For this case the concentration of water in Equation (14) shall be taken as weight fraction of water within the heat exchange volume: protein + droplet + δ

layer of solvent, $w_{HE\,water}$. It can be estimated as: $w_{HE\,water} = \frac{(r^3 - r_p{}^3)\rho_{water}}{((r+\delta)^3 - r^3)\rho_{iso} + (r^3 - r_p{}^3)\rho_{water}}$.

If we assume that the increase in concentration of water does not affect the number of droplets but results in increase of their size only and that each of the droplets contains one protein molecule, the radius of the droplet can be linked with concentration of water in the mixture as: $r = \sqrt[3]{r_p{}^3 + (r_0{}^3 - r_p{}^3)\frac{w_{water}(1-w_{water\,0})}{w_{water\,0}(1-w_{water})}}$, where r_0 the size of the droplets at concentration of water $w_{water\,0}$. For a given r_p and r_0 at $w_{water\,0}$ the value of $w_{HE\,water}$ can be calculated and used with Equation (14) to obtain the compressibility of protein as function of concentration of water in the system for any given value of δ. The value of δ can be varied to obtain the best fitting of calculated and experimental compressibilities. For r_p = 2nm (variation of this value by 100% has a minor effect on the results) and r_0 = 7nm (5nm of thickness of layer of water) at w_0 =0.075 the value of δ is 20nm. This is a reasonable estimate for the 'effective' thickness of the layer of solvent around the water droplets participating in the heat exchange. The continuous line in the Figure 4(a) represents the predicted dependence of apparent compressibility of proteins on concentration of water in microemulsion for the above parameters. The predicted dependence describes well the experimental data. An increase in the radius of droplet, r_0, will result in higher values for δ corresponding to the experiments data. Overall, the above estimations demonstrate an importance of examination of the heat exchange between the solvent and the interior of nano-particles when describing the effects of encapsulation on the measured compressibility of the encapsulated material. Detailed analysis of intrinsic compressibility of encapsulated material in AOT w/o microemulsions measured at one frequency requires knowledge of size and, perhaps, other the structural attributes of the droplets. Measurements of compressibility at different frequencies, combined with the measurements of ultrasonic attenuation, have a potential of providing the required information.

10. Ultrasonic monitoring of enzyme reactions in microemulsions

Previously it was shown that high-resolution ultrasonic spectroscopy can be applied for real-time monitoring of enzyme reactions in a wide range of concentrations and substrates. The technique does not require optical transparency, optical markers or secondary reactions and allows real-time non-invasive measurements. The capability of this and other ultrasonic techniques were demonstrated for a variety of reactions catalysed by enzymes, namely, urease, α-amylase and catalase (Kudryashov et. al, 2003), chymosin (Dwyer et al., 2005) proteinase K (Buckin & Craig, 2005), invertase (Resa et al, 2009), and cellobiase (Resa & Buckin, 2011) as well as other types of bioprocesses (McClements, 1995; Povey, 1997). It provided the detailed reaction extent and rate profiles in a broad range of concentrations, allowed analysis of the reverse reaction, determination of equilibrium constant and of the molar Gibbs free energy of reactions as well as analysis of reactions kinetic models (Resa & Buckin, 2011). Figure 4(b) illustrates our results for the real-time ultrasonic monitoring of activity enzyme, β-glucosidase, in aqueous solution (10 mM sodium acetate buffer, pH 4.90) and encapsulated in IPM microemulsion (50:50 w/w ratio of oil to surfactant+cosurfactant) at 24% water in the presence of substrate, cellobiose (disaccharide). The concentration of water in microemulsion corresponds to the part of ultrasonic microemulsion phase diagram,

where a presence of water droplets with significant size of the water pool was identified previously (Hickey et al., 2006). This provides some hydration level for encapsulated molecules of enzyme and the substrate. The reaction was started by adding of concentrated solution of enzyme to microemulsion or to the aqueous solution with the substrate. The concentrations of the enzyme and the substrate in aqueous phase of microemulsion were the same as in the aqueous solution. The time profiles for ultrasonic velocity are presented in the Figure 4(b) (main frame – aqueous solution, insert – microemulsion).

In aqueous solutions at our concentrations β-glucosidase provides hydrolysis of cellobiose, during which β-1,4-glycosidic bond is cleaved, one molecule of water is absorbed, and two D-glucose molecules are released. This causes a change in the compressibility and density of the solution, thus resulting in a change of ultrasonic velocity. The ultrasonic reaction time profiles can be recalculated into the reaction extent profile, $\zeta(t) = \frac{w_C^0 - w_C(t)}{w_C^0}$, where w_C^0 and $w_C(t)$ are the concentrations of cellobiose at time zero and at time t. This requires the concentration increment of ultrasonic velocity of the reaction, Δa_u, which represents the relative change of ultrasonic velocity caused by conversion of the reactants into products, calculated per unit of concentration of the reactant (cellobiose) converted (Resa & Buckin, 2011). It is linked with the reaction extent as: $\zeta(t) = \frac{u(t) - u^0}{u_0 \Delta a_u w_C^0}$, where $u(t)$ and u^0 are the ultrasonic velocities at reaction time t and time zero, and u_0 is the ultrasonic velocity in the solvent (solution or microemulsion without the components of the reaction). For hydrolysis of cellobiose $\Delta a_u = a_{uG} \frac{2M_G}{M_C} - a_{uC} - a_{uW} \frac{M_W}{M_C}$, where M represents the molar mass of a particular component and symbols G, W and C stand for glucose, water and cellbiose (Resa & Buckin, 2011). The value of a_{uW} is the concentration increment of ultrasonic velocity of water added to microemulsion in the amount consumed by the reaction. For our conditions in microemulsion this addition corresponds to the change in concentration of water by 0.03% of total 24% and therefore a_{uW} represents the partial concentration increment of water, $\bar{a}_u$. The same is true for the reaction in aqueous solution. We have measured the values of a_{uG}, a_{uW} and a_C in our aqueous solution for concentrations utilised in our reaction. This provided $\Delta a_u = 0.041$, which is close to value previously obtained for 50°C (Resa & Buckin, 2011). The reaction extent, $\zeta(t)$, for reaction in aqueous solution is represented by the right Y scale of the Figure 4(b).

In contrary to the aqueous solution, the reaction in microemulsion is accompanied by a decrease in ultrasonic velocity, however on a significantly smaller scale. Equation (25) can be used to recalculate the value of Δa_u for the aqueous solution to the value of Δa_u in IPM system if the values of φV, φE, φC_P and the physical properties of the continuous medium are known. We have used the data of (Banipal et al., 1997) on the apparent heat capacities at 25°C and the temperature slopes of the apparent volumes of cellobiose and glucose in water at infinite dilution and also the value of a_{uW} in microemulsion obtained in our titration measurements to estimate Δa_u for hydrolysis of cellobiose in IPM microemulsion (the physical properties if IPM system were taken from Hickey et.al., 2006). These estimations provided positive values of Δa_u. Our direct measurements of the difference in ultrasonic

Physical properties at 25°C	Water [a]	EO system[b] (80:20 w/w oil to surfactant ratio)	IPM system[c] (60:40w/w oil to surfactant and cosurfactant ratio)	0.1M AOT in Isooctane	Isooctane	Protein
Specific adiabatic compressibility (x10^{13}), $m^3\,kg^{-1}\,Pa^{-1}$	4.491	6.385	7.655	16.65[d]	18.12[d]	1.655[f]
Specific volume (x10^3), m^3kg^{-1}	1.003	1.109	1.158	1.437[d]	1.457[d]	0.662[f]
Thermal conductivity, $W\,m^{-1}\,K^{-1}$	0.5952	0.12	0.19	0.095[e]	0.095[e]	-
Specific thermal expansibility (×10^6) $m^3kg^{-1}\,K^{-1}$	0.257	0.827	0.982	1.97[d]	2.076	0.07[f]
Specific heat capacity, $J\,kg^{-1}\,K^{-1}$	4180	1686	1405	2037[e]	2037[e]	1403[g]
Viscosity, Pa s(×10^3)	0.890	17.2	8.6	0.516 [d]	0.479 [d]	-

[a] Handbook of Chemistry and Physics, 2004-2005; [b] Calculated from (Hickey et al., 2010) and (Pratas et al., 2010); [c] Calculated from (Hickey et al., 2006); [d] (Go´mez-Dı´az et al., 2006); [e] value for isooctane Handbook of Chemistry and Physics 2004-2005; [f] Taken as intrinsic characteristics of globular proteins (Chalikian, 2003); g] Calculated from (Privalov & Dragan, 2007) as average value for three globular proteins: cytochrome C, myoglobin and lysozyme.

Table 1. Physical properties of the media used in calculations.

velocity between microemulsion containing cellobiose (at the its initial concentration in our reaction) and glucose (at concentration corresponding 100% hydrolysis of cellobiose) as well as our data for a_{uW} in microemulsion provided $\Delta a_u \cong 0.005$. This corresponds to 0.04 m/s increase of ultrasonic velocity for 100% of hydrolysis of cellobiose in our microemulsion. The positive sign of Δa_u contradicts to the observed decrease of ultrasonic velocity in the reaction. Two possible explanation of this result can be suggested. 1) The physical state of cellobiose and glucose in microemulsions containing both of these molecules and the enzyme is significantly different than in microemulsions containing glucose and celobiose separately. It may results in the different sign for Δa_u at intermediate degrees of hydrolysis of cellobiose. This option can be verified or excluded through the measurements of ultrasonic velocity in microemulsions containing both components of the reaction. 2) The reaction observed in microemulsion is not the hydrolysis of cellobiose. We can speculate that an alternative reaction is related to transglycosylation activity of some of β-glucosidases resulting in production of tri- and tetrasaccharides. The activity can be enhanced by immobilisation and limited hydration (example: Chen & Ou-Yang, 2004; Marico et al., 2001), which are well known factors affecting functioning of enzymes in microemulsions (Kolisis & Stamatis, 2010). This could explain the observed decrease in ultrasonic velocity. Different energetics (free energy) of reactions of synthesis and hydrolysis of oligosaccharides in microemulsion as compared with aqueous solution can be another contributor. As can be seen from the Figure 4(b) the reaction time in the microemulsion is significantly shorter than in the aqueous solution. The reaction did not produce any substantial change in ultrasonic attenuation; neither a dispersion of velocity in the measured frequency range, 2 to 12 MHz, thus demonstrating that the structure of the microemulsion was not affected by the reaction.

11. Conclusions

High-resolution measurements of ultrasonic velocity and attenuation and their dependence on frequency allow analysis of a range of characteristics of microemulsion systems. This includes determination of phase diagrams, characterisation of size and state of microemulsion droplets and compounds encapsulated in them as well as real time monitoring of chemical reactions curried in microemulsions. Titration measurements with this technique allow identification of different 'sub-states' of microemulsion components, which can be utilised for upgrading the microemulsion phase diagram with additional 'sub phases' corresponding to different states of water and surfactant in microemulsions. Consideration of these 'sub phases' and their position on the phase diagram could be employed in design of w/o microemulsions designated for encapsulation of active ingredients (e.g. proteins), which require an appropriate level of hydration for their functioning. Quantitative analysis of compressibility of microemulsions and its molecular interpretation in most cases can be performed within the thermal low frequency limit approach, which provides direct thermodynamic relationships for concentration dependence of compressibility, and effects of continuous phase on compressibilities of components of microemulsions.

Acknowledgments: This research was supported by the MASAF315 grant from SFI Ireland. We are thankful to Evgeny Kudryashov for collaboration during this project and to Margarida Altas for her assistance in some measurements and preparation of manuscript.

12. References

Alany, R.G., Tucker, I.G., Davies, N.M., Rades, T. (2001). Characterising colloidal structures of pseudoternary phase diagrams formed by oil/water/amphiphile systems. *Drug Dev. Ind. Pharm.*, Vol.27, pp. 31–38.

Allegra, J.R., Hawley, S.A. (1972). Attenuation of sound in suspensions and emulsions: *theory and experiment. J. Acoust. Soc. Am.*, Vol.51, pp. 1545–1564

Amararene, A., Gindre, M., Le Hue´rou, J.Y., Nicot, C., Urbach, W., and Waks, M. (1997). Water Confined in Reverse Micelles: Acoustic and Densimetric Studies. *J. Phys. Chem. B*, Vol. 101, pp.10751-10756

Amararene, A., Gindre, M., Le Hue´rou, J.Y., Urbach, W., Valdez, D., & Waks, M. (2000). Adiabatic compressibility of AOT, sodium bis 2-ethylhexyl sulfosuccinate reverse micelles: Analysis of a simple model based on micellar size and volumetric measurements. *Physical review E.*, Vol. 61, No. 1 pp. 682-689

Austin, J.C., Holmes, A.K., Tebbutt, J.S., Challis, R.E. (1996). Ultrasonic wave propagation in colloid suspensions and emulsions: recent experimental results. *Ultrasonics,* Vol.34, pp. 369–374

Ballaro, S., Mallamace, F., Wanderlingh, F. (1980). Sound velocity and absorption inmicroemulsion. *Phys. Lett.*, Vol.77A, pp. 198–202

Banipal, P. K. , Banipal, T. S., Larkb B. S. and Ahluwaliaa, J. C. (1997). Partial molar heat capacities and volumes of some mono-, di- and tri-saccharides in water at 298.15, 308.15 and 318.15 K. *J. Chem. Soc., Faraday Trans.*, Vol.93, No.1, pp. 81-87

Buckin, V. (1988). Hydration of nucleic bases in dilute aqueous solutions. Apparent molar, adiabatic and isothermal compressibilities, apparent molar volumes and their temperature slopes at 25 ◦C. *Biophys. Chem.*, Vol.29, pp. 283–292

Buckin ,V., Smyth, C. (1999). High-resolution ultrasonic resonator measurements for analysis of liquids, *Sem. Food Anal.*, Vol.4, pp. 113–130

Buckin, V., Kudryashov, E. (2001). Ultrasonic shear wave rheology of weak particle gels, *Advances in Colloid and Interface Science*, Vol.89-90, pp. 401-422

Buckin, V., O'Driscoll B. (2002). Ultrasonic waves and material analysis: recent advances and future trends. *Lab. Plus Int.,* Vol.16 (3), pp. 17–21

Buckin, V. & Craig, E. (2005). New applications of high resolution ultrasonic spectroscopy for real time analysis of enzymatic proteolysis, *European BioPharma Review (Summer),* pp. 50 - 53

Cao Y.N., Diebold G.J., Zimmt M.B. (1997). Transient grating studies of ultrasonic attenuation in reverse micellar solutions, *Chemical Physics Letters,* Vol.276, p.p. 388-392

Chalikian, T. (2003). Volumetric Properties of Proteins. *Ann. Rev. Biophys. Biomol. Struct*, Vol. 32, pp.207–35

Chen, C.W. & Chao-Chih Ou-Yang, C.-C. (2004). Bounded water kinetic model of beta-galactosidase in reverse micelles. *Bioprocess Biosyst. Eng.* Vol. 26, pp. 307–313

Choi, Y. and Okos, M.R. (1986). Effects of Temperature and Composition on the Thermal Properties of Foods . *Journal of Food Process and Applications,*Vol. 1(1). pp. 93–101

Coupland, J.N., McClements, J.D., (2001). Droplet size determination in food emulsions: comparison of ultrasonic and light scattering methods. *J. Food Eng*., Vol.50, pp.117–120

Dwyer, C., Donnelly, L., Buckin V. (2005). Ultrasonic analysis of rennet-induced pre-gelation and gelation processes in milk, *J. Dairy Res.* Vol.72, pp. 303–310

Epstein, P.S., Carhart, R.J. (1953). The absorption of sound in suspensions and emulsions.I. Water fog in air. *J. Acoust. Soc. Am.* Vol.25, pp.553–562

Go´mez-Dı´az, Mejuto D., and NavazaJ. M. (2006). Density, Viscosity, and Speed of Sound of Solutions of AOT Reverse Micelles in2,2,4-Trimethylpentane, *J. Chem. Eng. Data*, Vol.51, pp. 409-411

Handbook of Chemistry and physics, 85th edition *CRC press*, 2004-2005

Hasegawa, M., Sugimura,T., Suzaki, Y., and Yoichi Shindo, Y. (1994). Microviscosity in Water Pool of Aerosol-OT Reversed Micelle Determined with Viscosity-Sensitive Fluorescenck Probe, Auramine 0, and Fluorescence Depolarization of Xanthene Dyes. *J. Phys. Chem*. Vol. 98, pp. 2120-2124

Hemar, Y., Hocquart, R. And Palierne, J. F. (1998). Frequency-dependent compressibility in emulsions: Probing interfaces using Isakovich's sound absorption, *Europhys. Lett*., Vol.42 (3), pp. 253-258

Hickey, S., Lawrence, M.J., Hagan, S.A., Buckin, V. (2006). Analysis of the Phase Diagram and Microstructural Transitions in Phospholipid Microemulsion Systems using High-Resolution Ultrasonic Spectroscopy, *Langmuir*, Vol.22, pp. 5575-5583

Hickey, S., Lawrence, M. J., Hagan, S.A., Kudryashov, E., Buckin, V. (2010). Analysis of Phase Diagram and Microstructural Transitions in an Ethyl Oleate/Water/Tween 80/Span 20 Microemulsion System using High-Resolution Ultrasonic Spectroscopy, *International Journal of Pharmaceutics* Vol. 388, pp. 213–222

Isakovich M. A., Zh. (1948). *Eksp. Teor.Fiz*., Vol. 18, pp. 907-912

Kaatze, U., Hushcha, T. O. & Eggers, F. (2000). Ultrasonic Broadband Spectrometry of Liquids: A Research Tool in Pure and Applied Chemistry and Chemical Physics, *J. Solution Chemistry,* Vol. 29, No. 4, pp. 299-368

Kolisis, F. N. & Stamatis, H. (2010). REVERCE MICELLES, ENZYMES, *Encyclopedia of Industrial Biotechnology: Bioprocess, Bioseparation, and Cell Technology,* ed M. C. Flickinger, John Wiley & Sons, Inc.

Kudryashov E., Smyth C., O'Driscoll B., Buckin, V. (2003). High-Resolution Ultrasonic Spectroscopy for analysis of chemical reactions in real time, *Spectroscopy* Vol.18 (10), pp. 26–32

Lang, J., Djavanbakht, A., Zana, R. (1980). Ultrasonic absorption study of microemulsions in ternary and pseudoternarnary systems. *J. Phys. Chem.* Vol. 84, pp.1541–1547

Letamendia, L., Pru-Lestret, E., Panizza, P., Rough, J., Scioritino, F., Tartaglia, P., Hashimoto, C., Ushiki, H., Risso, D. (2001). Relaxation phenomena in AOT–water–decane critical and dense microemulsions. *Physica A*,Vol.300, pp. 53–81

Litovitz, T.A. and Davis, C.M. (1964). Structural and Shear relaxation in Liquids. In *Physical Acoustic*, Vol.2, Part A, Ed. W.P. Mason, pp. 282-349, Academic Press, NY

Title;Effective Transglycosylation catalyzed by a Lipid-coated Glycosidase in Water-containing Supercritical Fluoroform.

Marico, F., Toshiaki, M., & Yoshio, O. (2001). Effective Transglycosylation catalyzed by a Lipid-coated Glycosidase in Water-containing Supercritical Fluoroform. *Nippon Kagakkai Koen Yokoshu*, Vol.79, No.2, pp.931, ISSN:0285-7626

McClements, (1995). Advances in the application of ultrasound in food analysis and processing. *Trends in Food Science and Technology*, Vol.6 pp. 293-299

Mehta, S.K., Kawaljit. (1998). Isentropic compressibility and transport properties of CTAB–alkanol–hydrocarbon–water microemulsion systems. *Colloids Surf. A*, Vol.136, pp. 35–41

Morse, P.M. & Ingard, K.U. (1986). *Theoretical Acoustic*, Princeton University Press

Pierce, A. D. (1991). *Acoustics*, Acoustical Society of America, NY.

Povey M.J. (1997). Ultrasonic Techniques for Fluid Characterisation, *Academic Press, London*

Pratas, M. J., Freitas S., Oliveira, M. B., Monteiro, S. C., Lima, A.S., and Coutinho, J. A. P. (2010). Densities and Viscosities of Fatty Acid Methyl and Ethyl Esters. *J. Chem. Eng. Data*, Vol.55, pp. 3983–3990

Privalov, P. L. & Dragan, A.I. (2007). Microcalorimetry of biological macromolecules. *Biophysical Chemistry*, Vol.126, pp. 16–24

Resa, P., Elvira, L., Sierra, C., Montero de Espinosa, F. (2009). Ultrasonic velocity assay of extracellular invertase in living yeasts. *Anal.Biochem.*, Vol.384, pp. 68–73

Resa P. & Buckin V. (2011). Ultrasonic analysis of kinetic mechanism of hydrolysis of cellobiose by beta-glucosidase. *Analytical Biochemistry,* Vol.415, pp. 1–11

Smyth, C., Kudryashov, E., Buckin, V. (2001). High-frequency shear and volume viscoelastic moduli of casein particle gel. *Colloids and Surfaces, A: Physicochemical and Engineering Aspect*s, Vol.183–185, pp. 517–526

Spehr, T.L. (2010). Water Dynamics in Soft Confinement-Neutron Scattering Investigation of Reverse Micelles. *Technical University of Darmstadt*. PhD. Thesis, Darmstadt, D17

Thurston, R.N. (1964). *Physical Acoustics: Principles and Methods*, Academic Press, New York, Mason, W.P. (Eds.), vol.1, part A, ch. 1

Valdez, D., Le Hue´ rou, J Y., Gindre, M., Urbach, W., and Waks, M. (2001). Hydration and Protein Folding in Water and in Reverse Micelles: Compressibility and Volume Changes *Biophysical Journal* , Vol.80, pp.2751–2760

Van Dijk, M., Joosten, J., Levine ,Y., and Bedeaux, D. (1989). *J. Phys. Chem*. Vol.93, pp. 2506-2512

Vasquez, V. R., Williams, B. C., & Graeve, O. A. (2011). Stability and Comparative Analysis of AOT/Water/Isooctane Reverse Micelle System Using Dynamic Light Scattering and Molecular Dynamics. *J. Phys. Chem. B*. Vol. 115, pp. 2979–2987

Wines, T.H., Dukhin, A., Somasundaran, P. (1999). Acoustic spectroscopy for characterizing heptane/H_2O/AOT reverse microemulsions. *J. Colloid Interface Sci*., Vol.216, pp.303–308

Waterman, P.C., Truell, R. (1961). Multiple scattering of waves. *J. Math. Phys.,* Vol.2, pp. 512–537

Yoshimura, Y., Abe, I., Ueda, M., Kajiwara K., Hori T., Schelly, Z. (2000). Apparent Molar Volume of Solubilized Water in AOT/Isooctane/Water Reverse Micellar Aggregates. *Langmuir*, Vol.16, pp.3633-3635

Zana, R., Lang, J., Sorba, O., Cazabat , A.M., Langevin, D. (1982). Ultrasonic investigation of critical behaviour and percolation phenomena in microemulsions. *Journal de Physique Lettres*, Vol.43, pp. 829-837

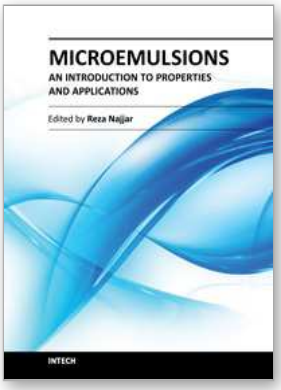

Microemulsions - An Introduction to Properties and Applications

Edited by Dr. Reza Najjar

ISBN 978-953-51-0247-2
Hard cover, 250 pages
Publisher InTech
Published online 16, March, 2012
Published in print edition March, 2012

The rapidly increasing number of applications for microemulsions has kept this relatively old topic still at the top point of research themes. This book provides an assessment of some issues influencing the characteristics and performance of the microemulsions, as well as their main types of applications. In chapter 1 a short introduction about the background, various aspects and applications of microemulsions is given. In Part 2 some experimental and modeling investigations on microstructure and phase behavior of these systems have been discussed. The last two parts of book is devoted to discussion on different types of microemulsion's applications, namely, use in drug delivery, vaccines, oil industry, preparation of nanostructured polymeric, metallic and metal oxides materials for different applications.

InTech Europe
University Campus STeP Ri
Slavka Krautzeka 83/A
51000 Rijeka, Croatia
Phone: +385 (51) 770 447
Fax: +385 (51) 686 166
www.intechopen.com

InTech China
Unit 405, Office Block, Hotel Equatorial Shanghai
No.65, Yan An Road (West), Shanghai, 200040, China
中国上海市延安西路65号上海国际贵都大饭店办公楼405单元
Phone: +86-21-62489820
Fax: +86-21-62489821